The Star Formation Newsletter

A community newsletter on Star and Planet Formation research

No. 368 — 31 August 2023

Editor: João Alves www.starformation.news

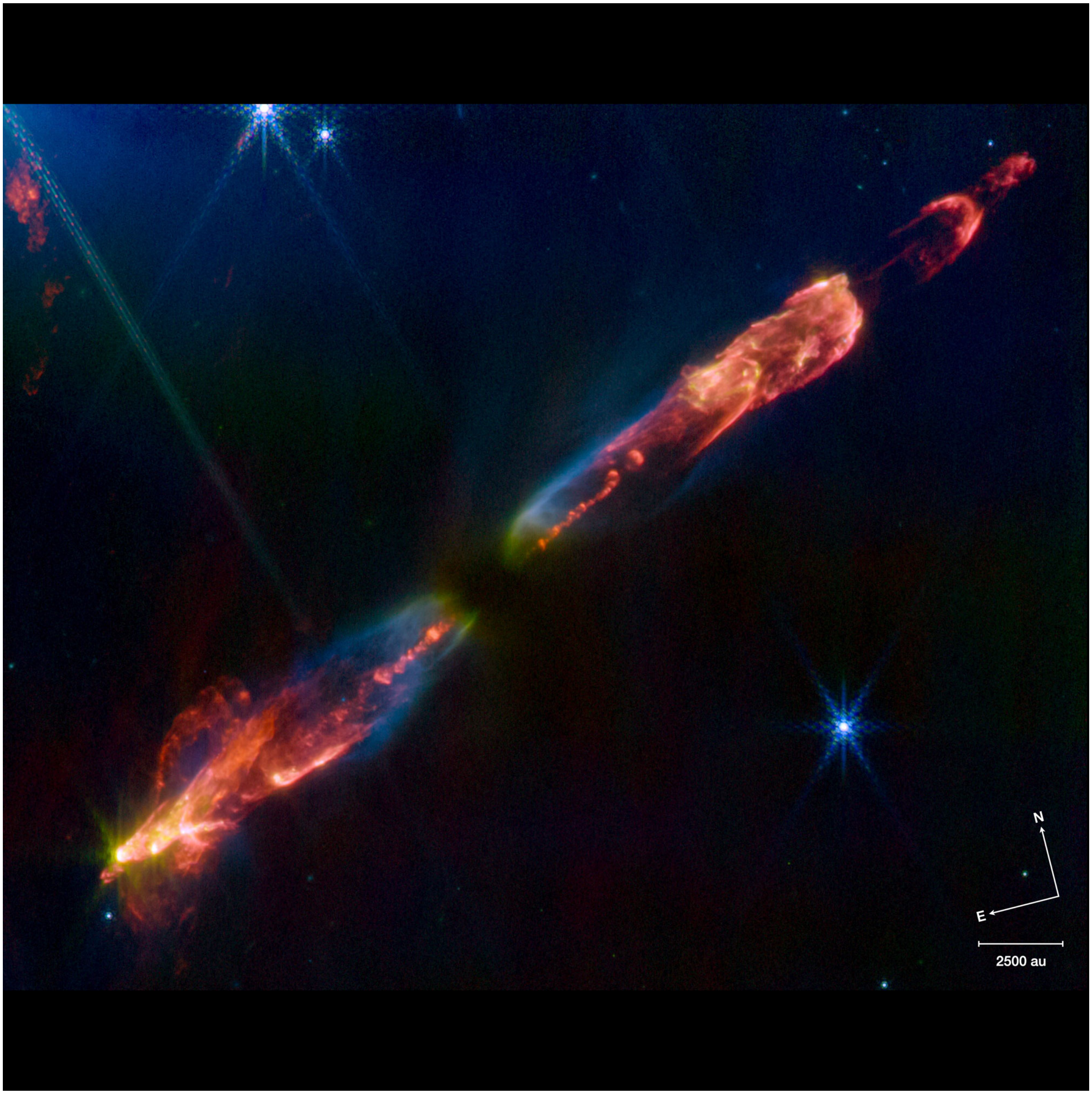

Cover image caption

A three-colour JWST NIRCam composite of the bipolar HH 211 outflow, in the Perseus molecular, not far from the young stellar cluster IC348. The composite consists of images made in the F335M (blue), F460M (green) and F470N (red) filters. The data shows a surprising absence of atomic or ionized emission, suggesting that the jet's core is primarily molecular. The orientation and projected scale in astronomical units (au) assuming a distance of 321 pc are shown in the lower right corner.

Credits: NASA, ESA, CSA - Ray et al. 2023.

Note from the Editor

The Star Formation Newsletter is now on the web at **www.starformation.news**. This PDF file contains the monthly Abstracts and links. Red text in this PDF is a url link. Submitting an abstract to the SFN is as simple as entering the arXiv ID (e.g., 2006.10139) in a web form on the SFN web site. **Do not remove the LaTeX formatting when submitting to the arXiv**. If you do, your abstract will not look great either at the arXiv or the SFN.

Abstracts

1. Spectral survey of a Hot core with an Eruptive Accretion in S255IR NIRS3 (SHEA): The discovery of class I and class II millimeter methanol maser transitions

Giseon Baek, Jeong-Eun Lee, Neal J. Evans II, Tomoya Hirota, Yuri Aikawa, Ji-hyun Kang, Jungha Kim, Jes K. Jørgensen ★ We report the detection of the millimeter CH_3OH masers including a new detection of class I ($11_{0,11}$-$10_{1,10}$A) and class II ($6_{1,5}$-$5_{2,4}$E) maser transitions toward the high-mass protostar S255IR NIRS3 in post-burst phase. The CH_3OH emissions were detected as a mixture of maser and thermal characteristics. We examine the detected transitions using an excitation diagram and LTE model spectra and compare the observed properties with those of thermal lines. Class II CH_3OH maser transitions showed distinctive intensity and velocity distributions from those of thermal transitions. Bright distinct emission components in addition to the fragmented and arc-shaped emissions are only detected in class I CH_3OH maser transitions toward southern and western directions from the protostellar position, implying the presence of the slow outflow shocks.

2. Isolating Dust and Free-Free Emission in ONC Proplyds with ALMA Band 3 Observations

Nicholas P. Ballering, L. Ilsedore Cleeves, Thomas J. Haworth, John Bally, Josh A. Eisner, Adam Ginsburg, Ryan D. Boyden, Min Fang, Jinyoung Serena Kim ★ The Orion Nebula Cluster (ONC) hosts protoplanetary disks experiencing external photoevaporation by the cluster's intense UV field. These "proplyds" are comprised of a disk surrounded by an ionization front. We present ALMA Band 3 (3.1 mm) continuum observations of 12 proplyds. Thermal emission from the dust disks and free-free emission from the ionization fronts are both detected, and the high-resolution (0.057") of the observations allows us to spatially isolate these two components. The morphology is unique compared to images at shorter (sub)millimeter wavelengths, which only detect the disks, and images at longer centimeter wavelengths, which only detect the ionization fronts. The disks are small (r_d = 6.4–38 au), likely due to truncation by ongoing photoevaporation. They have low spectral indices ($\alpha \lesssim 2.1$) measured between Bands 7 and 3, suggesting the dust emission is optically thick. They harbor tens of Earth masses of dust as computed from the millimeter flux using the standard method, although their true masses may be larger due to the high optical depth. We derive their photoevaporative mass-loss rates in two ways: first, by invoking ionization equilibrium, and second using the brightness of the free-free emission to compute the density of the outflow. We find decent agreement between these measurements and $\dot{M} = 0.6$–$18.4 \times 10^{-7}\ M_\odot\ \mathrm{yr}^{-1}$. The photoevaporation timescales are generally shorter than the $\sim$1 Myr age of the ONC, underscoring the known "proplyd lifetime problem." Disk masses that are underestimated due to being optically thick remains one explanation to ease this discrepancy.

3. Tracing snowlines and C/O ratio in a planet-hosting disk: ALMA molecular line observations towards the HD169142 disk

Alice S. Booth, Charles J. Law, Milou Temmink, Margot Leemker, Enrique Macias ★ The composition of a forming planet is set by the material it accretes from its parent protoplanetary disk. Therefore, it is crucial to map the chemical make-up of the gas in disks to understand the chemical environment of planet formation. This paper presents molecular line observations taken with the Atacama Large Millimeter/submillimeter Array of the planet-hosting disk around the young star HD 169142.

We detect N2H+, CH3OH, [CI], DCN, CS, C34S, 13CS, H2CS, H2CO, HC3N and c-C3H2 in this system for the first time. Combining these data with the recent detection of SO and previously published DCO+ data, we estimate the location of H2O and CO snowlines and investigate radial variations in the gas phase C/O ratio. We find that the HD 169142 disk has a relatively low N2H+ flux compared to the disks around Herbig stars HD 163296 and MWC 480 indicating less CO freeze-out and place the CO snowline beyond the millimetre disk at 150 au. The detection of CH3OH from the inner disk is consistent with the H2O snowline being located at the edge of the central dust cavity at 20 au. The radially varying CS/SO ratio across the proposed H2O snowline location is consistent with this interpretation. Additionally, the detection of CH3OH in such a warm disk adds to the growing evidence supporting the inheritance of complex ices in disks from the earlier, colder stages of star formation. Finally, we propose that the giant HD 169142 b located at 37 au is forming between the CO2 and H2O snowlines where the local elemental make of the gas is expected to have C/O=1.0.

4. Chemical evolution of some selected complex organic molecules in low-mass star-forming regions

Bratati Bhat, Rumela Kar, Suman Kumar Mondal, Rana Ghosh, Prasanta Gorai, Takashi Shimonishi, Kei E. I. Tanaka, Kenji Furuya, Ankan Das ★ The destiny of complex organic molecules (COMs) in star-forming regions is interlinked with various evolutionary phases. Therefore, identifying these species in diversified environments of identical star-forming regions would help to comprehend their physical and chemical heritage. We identified multiple COMs utilizing the Large Program 'Astrochemical Surveys At IRAM' (ASAI) data, dedicated to chemical surveys in Sun-like star-forming regions with the IRAM 30 m telescope. It was an unbiased survey in the millimetre regime, covering the prestellar core, protostar, outflow region, and protoplanetary disk phase. Here, we have reported some transitions of seven COMs, namely, methanol (CH3OH), acetaldehyde (CH3CHO), methyl formate (CH3OCHO), ethanol (C2H5OH), propynal (HCCCHO), dimethyl ether (CH3OCH3), and methyl cyanide (CH3CN) in some sources L1544, B1-b, IRAS4A, and SVS13A. We found a trend among these species from the derived abundances using the rotational diagram method and MCMC fit. We have found that the abundances of all of the COMs, except for HCCCHO, increase from the L1544 (prestellar core) and peaks at IRAS16293-2422 (class 0 phase). It is noticed that the abundance of these molecules correlate with the luminosity of the sources. The obtained trend is also visible from the previous interferometric observations and considering the beam dilution effect.

5. The potential of VLTI observations for the study of circumstellar disk variability

A. Bensberg, J. Kobus, S. Wolf ★ Context. A characteristic feature of young stellar objects is their variability, which is caused by a variety of different physical processes. High-resolution interferometric observations in the near- and mid-infrared wavelength ranges spanning multiple epochs allow the detailed study of these processes. Aims. We aim at investigating the expected variations of the interferometric observables connected to changes in the measured photometric fluxes of a typical variable accreting central young stellar object with a circumstellar disk. Methods. We calculated visibilities and closure phases as well as the photometric flux of brightness distributions obtained using 3D Monte Carlo radiative transfer simulations for a model of a circumstellar disk with an accreting central star. Results. Changes in the accretion luminosity of the central object, that is, an accreting pre-main-sequence star, can lead to significant variations in the visibility and closure phase of the star-disk system measured with instruments at the Very Large Telescope Interferometer (VLTI) that can be related to changes in the photometric flux. Taking into account additional effects due to baseline variation, interferometric observations can provide valuable contributions to the understanding of the underlying processes. Additionally, we provide the web application VLTI B-VAR that allows the impact of the hour angle on the visibility and closure phase for customized intensity maps to be estimated.

6. Forming Gas Giants Around a Range of Protostellar M-dwarfs by Gas Disk Gravitational Instability

Alan P. Boss, Shubham Kanodia ★ Recent discoveries of gas giant exoplanets around M-dwarfs (GEMS) from transiting and radial velocity (RV) surveys are difficult to explain with core-accretion models. We present here a homogeneous suite of 162 models of gravitationally unstable gaseous disks. These models represent an existence proof for gas giants more massive than 0.1 Jupiter masses to form by the gas disk gravitational instability (GDGI) mechanism around M-dwarfs for comparison with observed exoplanet demographics and protoplanetary disk mass estimates for M-dwarf stars. We use the Enzo 2.6 adaptive mesh refinement (AMR) 3D hydrodynamics code to follow the formation and initial orbital evolution of gas giant protoplanets in gravitationally unstable gaseous disks in orbit around M-dwarfs with stellar masses ranging from 0.1 $M_\odot$ to 0.5 $M_\odot$. The gas disk masses are varied over a range from disks that are too low in mass to form gas giants rapidly to those where numerous gas giants are formed, therefore revealing the critical disk mass necessary for gas giants to form by the GDGI mechanism around M-dwarfs. The disk masses vary from 0.01 $M_\odot$ to 0.05 $M_\odot$ while the disk to star mass ratios explored range from 0.04 to 0.3. The models have varied initial outer disk temperatures (10 K to 60 K) and varied levels of AMR grid spatial resolution, producing a sample of expected gas giant protoplanets for each star mass. Broadly speaking, disk masses of at least 0.02 $M_\odot$ are needed for the GDGI mechanism to form gas giant protoplanets around M-dwarfs.

7. HH 80/81: Structure and Kinematics of the Fastest Protostellar Outflow

John Bally, Bo Reipurth ★ Hubble Space Telescope images obtained in 2018 are combined with archival HST data taken in 1995 to detect changes and measure proper motions in the HH 80/81 shock complex which is powered by the fastest known jet driven by a forming star, the massive object IRAS 18162-2048. Some persistent features close to the radio jet axis have proper motions grater than 1,000 km/s away from IRAS 18162-2048. About 3 to 5 parsecs downstream from the IRAS source and beyond HH 80/81, H-alpha emission traces the rim of a parsec-scale bubble blown by the jet. Lower speed motions are seen in [Sii] away from the jet axis; these features have a large component of motion at right-angles to the jet. We identify new HH objects and H2 shocks in the counterflow opposite HH 80/81. The northeastern counterflow to HH 80/81 exhibits an extended but faint complex of 2.12 um H2 shocks. The inner portion of the outflow is traced by dim 1.64 um [Feii] emission. The full extent of this outflow is at least 1,500" (about 10 pc in projection at a distance of 1.4 kpc). We speculate about the conditions responsible for the production of the ultra-fast jet and the absence of prominent large-scale molecular outflow lobes.

8. A Keplerian disk with a four-arm spiral birthing an episodically accreting high-mass protostar

R. A. Burns, Y. Uno, N. Sakai, J. Blanchard, Z. Rosli, G. Orosz, Y. Yonekura, Y. Tanabe, K. Sugiyama, T. Hirota, Kee-Tae Kim, A. Aberfelds, A. E. Volvach, A. Bartkiewicz, A. Caratti o Garatti, A. M. Sobolev, B. Stecklum, C. Brogan, C. Phillips, D. A. Ladeyschikov, D. Johnstone, G. Surcis, G. C. MacLeod, H. Linz, J. O. Chibueze, J. Brand, J. Eislöffel, L. Hyland, L. Uscanga, M. Olech, M. Durjasz, O. Bayandina, S. Breen, S. P. Ellingsen, S. P. van den Heever, T. R. Hunter, X. Chen ★ High-mass protostars ($M_\star > 8\ M_\odot$) are thought to gain the majority of their mass via short, intense bursts of growth. This episodic accretion is thought to be facilitated by gravitationally unstable and subsequently inhomogeneous accretion disks. Limitations of observational capabilities, paired with a lack of observed accretion burst events has withheld affirmative confirmation of the association between disk accretion, instability and the accretion burst phenomenon in high-mass protostars. Following its 2019 accretion burst, a heat-wave driven by a burst of radiation propagated outward from the high-mass protostar G358.93-0.03-MM1. Six VLBI (very long baseline interferometry) observations of the raditively pumped 6.7 GHz methanol maser were conducted during this period, tracing ever increasing disk radii as the heat-wave propagated outward. Concatenating the VLBI maps provided a sparsely sampled, milliarcsecond view of the spatio-kinematics of the accretion disk covering a physical range of $\sim$ 50 - 900 AU. We term this observational approach 'heat-wave mapping'. We report the discovery of a Keplerian accretion disk with a spatially resolved four-arm spiral pattern around G358.93-0.03-MM1. This result positively implicates disk accretion and spiral arm instabilities into the episodic accretion high-mass star formation paradigm.

9. The Orion-Taurus ridge: a synchrotron radio loop at the edge of the Orion-Eridanus superbubble

Andrea Bracco, Marco Padovani, Juan D. Soler ★ Large-scale synchrotron loops are recognized as the main source of diffuse radio-continuum emission in the Galaxy at intermediate and high Galactic latitudes. Their origin, however, remains rather unexplained. Using a combination of multi-frequency data in the radio band of total and polarized intensities, for the first time in this letter, we associate one arc – hereafter, the Orion-Taurus ridge – with the wall of the most prominent stellar-feedback blown shell in the Solar neighborhood, namely the Orion-Eridanus superbubble. We traced the Orion-Taurus ridge using 3D maps of interstellar dust extinction and column-density maps of molecular gas, $N_{\rm H_2}$. We found the Orion-Taurus ridge at a distance of 400 pc, with a plane-of-the-sky extent of 180 pc. Its median $N_{\rm H_2}$ value is $(1.4^{+2.6}_{-0.6}) \times 10^{21}$ cm^{-2}. Thanks to the broadband observations below 100 MHz of the Long Wavelength Array, we also computed the low-frequency spectral-index map of synchrotron emissivity, β, in the Orion-Taurus ridge. We found a flat distribution of β with a median value of $-2.24^{+0.03}_{-0.02}$ that we interpreted in terms of depletion of low-energy (< GeV) cosmic-ray electrons in recent supernova remnants (10^5 - 10^6 yrs). Our results are consistent with plane-of-the-sky magnetic-field strengths in the Orion-Taurus ridge larger than a few tens of μG ($> 30 - 40\,\mu$G). We report the first detection of diffuse synchrotron emission from cold-neutral, partly molecular, gas in the surroundings of the Orion-Eridanus superbubble. This observation opens a new perspective to study the multiphase and magnetized interstellar medium with the advent of future high-sensitivity radio facilities, such as the C-Band All-Sky Survey and the Square Kilometre Array.

10. JWST reveals excess cool water near the snowline in compact disks, consistent with pebble drift

Andrea Banzatti, Klaus M. Pontoppidan, John Carr, Evan Jellison, Ilaria Pascucci, Joan Najita, Carlos E. Munoz-Romero, Karin I. Oberg, Anusha Kalyaan, Paola Pinilla, Sebastiaan Krijt, Feng Long, Michiel Lambrechts, Giovanni Rosotti, Gregory J. Herczeg, Colette Salyk, Ke Zhang, Edwin Bergin, Nick Ballering, Michael R. Meyer, Simon Bruderer, the JDISCS collaboration ★ Previous analyses of mid-infrared water spectra from young protoplanetary disks observed with the Spitzer-IRS found an anti-correlation between water luminosity and the millimeter dust disk radius observed with ALMA. This trend was suggested to be evidence for a fundamental process of inner disk water enrichment, used to explain properties of the Solar System 40 years ago, in which icy pebbles drift inward from the outer disk and sublimate after crossing the snowline. Previous analyses of IRS water spectra, however, were uncertain due to the low spectral resolution that blended lines together. We present new JWST-MIRI spectra of four disks, two compact and two large with multiple radial gaps, selected to test the scenario that water vapor inside the snowline is regulated by pebble drift. The higher spectral resolving power of MIRI-MRS now yields water spectra that separate individual lines, tracing upper level energies from 900 K to 10,000 K. These spectra clearly reveal excess emission in the low-energy lines in compact disks, compared to the large disks, demonstrating an enhanced cool component with $T \approx$ 170-400 K and equivalent emitting radius $R_{\rm eq} \approx$ 1-10 au. We interpret the cool water emission as ice sublimation and vapor diffusion near the snowline, suggesting that there is indeed a higher inwards mass flux of icy pebbles in compact disks. Observation of this process opens up multiple exciting prospects to study planet formation chemistry in inner disks with JWST.

11. CoCCoA: Complex Chemistry in hot Cores with ALMA. Selected oxygen-bearing species

Y. Chen, M. L. van Gelder, P. Nazari, C. L. Brogan, E. F. van Dishoeck, H. Linnartz, J. K. Jørgensen, T. R. Hunter, O. H. Wilkins, G. A. Blake, P. Caselli, K. -J. Chuang, C. Codella, I. Cooke, M. N. Drozdovskaya, R. T. Garrod, S. Ioppolo, M. Jin, B. M. Kulterer, N. F. W. Ligterink, A. Lipnicky, R. Loomis, M. G. Rachid, S. Spezzano, B. A. McGuire ★ Complex organic molecules (COMs) have been observed to be abundant in the gas phase toward protostars. Deep line surveys have been carried out only for a limited number of well-known high-mass star forming regions using the Atacama Large Millimeter/submillimeter Array (ALMA), which has unprecedented resolution and sensitivity. Statistical studies on oxygen-bearing COMs (O-COMs) in high-mass protostars using ALMA are still lacking. With the recent CoCCoA survey, we are able to determine the column density ratios of six O-COMs with respect to methanol (CH_3OH) in a sample of 14 high-mass protostellar sources to investigate their origin through ice and/or gas-phase chemistry. The selected species are: acetaldehyde (CH_3CHO), ethanol (C_2H_5OH), dimethyl ether (DME, CH_3OCH_3), methyl formate (MF, CH_3OCHO), glycolaldehyde (GA, CH_2OHCHO), and ethylene glycol (EG, $(CH_2OH)_2$). DME and MF have the highest and most constant ratios within one order of magnitude, while the other four species have lower ratios and exhibit larger scatter by 1-2 orders of magnitude. We compare the O-COM ratios of high-mass CoCCoA sources with those of 5 low-mass protostars available from the literature, along with the results from experiments and simulations. We find that the O-COM ratios with respect to methanol are on the same level in both the high- and low-mass samples, which suggests that these species are mainly formed in similar environments during star formation, probably in ice mantles on dust grains during early pre-stellar stages. Current simulations and experiments can reproduce most observational trends with a few exceptions, and hypotheses exist to explain the differences between observations and simulations/experiments, such as the involvement of gas-phase chemistry and different emitting areas of molecules.

12. New radio lobes at parsec scale from the East-West protostellar jet RAFGL2591

A. G. Cheriyan, S. Vig, Sreelekshmi Mohan ★ RAFGL2591 is a massive star-forming complex in the Cygnus-X region comprising of a cluster of embedded protostars and young stellar objects located at a distance of 3.33 kpc. We investigate low-frequency radio emission from the protostellar jet associated with RAFGL2591 using the Giant Metrewave Radio Telescope (GMRT) at 325, 610 and 1280 MHz. For the first time, we have detected radio jet lobes in the E-W direction, labelled as GMRT-1 and GMRT-2. While GMRT-1 displays a flat radio spectral index of α = -0.10 , GMRT-2 shows a steeply negative value α = -0.62 suggestive of non-thermal emission. H_2 emission maps show the presence of numerous knots, arcs and extended emission towards the East-West jet, excited by the protostar VLA 3. In addition, we report a few H_2 knots in the North-East and South-West for the first time. The radio lobes (GMRT-1, GMRT-2) and H_2 emission towards this region are understood in the context of the prominent East-West jet as well as its lesser-known sibling jet in the North-East and South-West direction. To model the radio emission from the lobes, we have employed a numerical model including both thermal and non-thermal emission and found number densities towards these lobes in the range 100 - 1000 cm^{-3} . The misalignment of the East-West jet lobes exhibits a reflection symmetry with a bending of $\sim$ 20$\circ$. We attempt to understand this misalignment through precession caused by a binary partner and/or a supersonic side wind from source(s) in the vicinity.

13. A magnetically driven disc wind in the inner disc of PDS 70

Justyn Campbell-White, Carlo F. Manara, Myriam Benisty, Antonella Natta, Rik A. B. Claes, Antonio Frasca, Jaehan Bae, Stefano Facchini, Andrea Isella, Laura Pérez, Paola Pinilla, Aurora Sicilia-Aguilar, Richard Teague ★ PDS 70 is so far the only young disc where multiple planets have been detected by direct imaging. The disc has a large cavity when seen at sub-mm and NIR wavelengths, which hosts two massive planets. This makes PDS 70 the ideal target to study the physical conditions in a strongly depleted inner disc shaped by two giant planets, and in particular to test whether disc winds can play a significant role in its evolution. Using X-Shooter and HARPS spectra, we detected for the first time the wind-tracing [O I] 6300AA line, and confirm the low-moderate value of mass-accretion rate in the literature. The [O I] line luminosity is high with respect to the accretion luminosity when compared to a large sample of discs with cavities in nearby star-forming regions. The FWHM and blue-shifted peak of the [O I] line suggest an emission in a region very close to the star, favouring a magnetically driven wind as the origin. We also detect wind emission and high variability in the He I 10830AA line, which is unusual for low-accretors. We discuss that, although the cavity of PDS 70 was clearly carved out by the giant planets, the substantial inner disc wind could also have had a significant contribution to clearing the inner-disc.

14. MagAO-X and HST high-contrast imaging of the AS209 disk at Hα

Gabriele Cugno, Yifan Zhou, Thanawuth Thanathibodee, Per Calissendorff, Michael R. Meyer, Suzan Edwards, Jaehan Bae, Myriam Benisty, Edwin Bergin, Matthew De Furio, Stefano Facchini, Jared R. Males, Laird M. Close, Richard D. Teague, Olivier Guyon, Sebastiaan Y. Haffert, Alexander D. Hedglen, Maggie Kautz, Andrés Izquierdo, Joseph D. Long, Jennifer Lumbres, Avalon L. McLeod, Logan A. Pearce, Lauren Schatz, Kyle Van Gorkom ★ The detection of emission lines associated with accretion processes is a direct method for studying how and where gas giant planets form, how young planets interact with their natal protoplanetary disk and how volatile delivery to their atmosphere takes place. Hα ($\lambda = 0.656\,\mu$m) is expected to be the strongest accretion line observable from the ground with adaptive optics systems, and is therefore the target of specific high-contrast imaging campaigns. We present MagAO-X and HST data obtained to search for Hα emission from the previously detected protoplanet candidate orbiting AS209, identified through ALMA observations. No signal was detected at the location of the candidate, and we provide limits on its accretion. Our data would have detected an Hα emission with $F_{\mathrm{H}\alpha} > 2.5 \pm 0.3 \times 10^{-16}$ erg s^{-1} cm^{-2}, a factor 6.5 lower than the HST flux measured for PDS70b (Zhou et al., 2021). The flux limit indicates that if the protoplanet is currently accreting it is likely that local extinction from circumstellar and circumplanetary material strongly attenuates its emission at optical wavelengths. In addition, the data reveal the first image of the jet north of the star as expected from previous detections of forbidden lines. Finally, this work demonstrates that current ground-based observations with extreme adaptive optics systems can be more sensitive than space-based observations, paving the way to the hunt for small planets in reflected light with extremely large telescopes.

15. ALMA-IMF VII – First release of the full spectral line cubes:Core kinematics traced by DCN J=(3-2)

N. Cunningham, A. Ginsburg, R. Galván-Madrid, F. Motte, T. Csengeri, A. M. Stutz, M. Fernández-López, R. H. Álvarez-Gutiérrez, M. Armante, T. Baug, M. Bonfand, S. Bontemps, J. Braine, N. Brouillet, G. Busquet, D. J. Díaz-González, J. Di Francesco, A. Gusdorf, F. Herpin, H. Liu, A. López-Sepulcre, F. Louvet, X. Lu, L. Maud, T. Nony, F. A. Olguin, Y. Pouteau, R. Rivera-Soto, N. A. Sandoval-Garrido, P. Sanhueza, K. Tatematsu, A. P. M. Towner, M. Valeille-Manet ★ ALMA-IMF is an Atacama Large Millimeter/submillimeter Array (ALMA) Large Program designed to measure the core mass function (CMF) of 15 protoclusters chosen to span their early evolutionary stages. It further aims to understand their kinematics, chemistry, and the impact of gas inflow, accretion, and dynamics on the CMF. We present here the first release of the ALMA-IMF line data cubes (DR1), produced from the combination of two ALMA 12m-array configurations. The data include 12 spectral windows, with eight at 1.3mm and four at 3mm. The broad spectral coverage of ALMA-IMF (6.7 GHz bandwidth coverage per field) hosts a wealth of simple atomic, molecular, ionised, and complex organic molecular lines. We describe the line cube calibration done by ALMA and the subsequent calibration and imaging we performed. We discuss our choice of calibration parameters and optimisation of the cleaning parameters, and we demonstrate the utility and necessity of additional processing compared to the ALMA archive pipeline. As a demonstration of the scientific potential of these data, we present a first analysis of the DCN (3-2) line. We find that DCN traces a diversity of morphologies and complex velocity structures, which tend to be more filamentary and widespread in evolved regions and are more compact in the young and intermediate-stage protoclusters. Furthermore, we used the DCN (3-2) emission as a tracer of the gas associated with 595 continuum cores across the 15 protoclusters, providing the first estimates of the core systemic velocities and linewidths within the sample. We find that DCN (3-2) is detected towards a higher percentage of cores in evolved regions than the young and intermediate-stage protoclusters and is likely a more complete tracer of the core population in more evolved protoclusters. The full ALMA 12m-array cubes for the ALMA-IMF Large Program are provided with this DR1 release.

16. The Role of Magnetic Fields in the Formation of the Filamentary Infrared Dark Cloud G11.11-0.12

Zhiwei Chen, Ramotholo Sefako, Yang Yang, Zhibo Jiang, Yang Su, Shaobo Zhang, Xin Zhou ★ We report on the near-infrared polarimetric observations of G11.11-0.12 (hereafter G11) obtained with SIRPOL on the 1.4 m IRSF telescope. The starlight polarisation of the background stars reveals the on-sky component of magnetic fields in G11, and these are consistent with the field orientation observed from polarised dust emission at $850\,\mu$m. The magnetic fields in G11 are perpendicular to the filament, and are independent of the filament's orientation relative to the Galactic plane. The field strength in the envelope of G11 is in the range $50 - 100\,\mu$G, derived from two methods. The analyses of the magnetic fields and gas velocity dispersion indicate that the envelope of G11 is supersonic but sub-Alfvénic. The critical mass-to-flux ratio in the envelope of G11 is close to 1 and increases to $\gtrsim 1$ on the spine of G11. The relative weights on the importance of magnetic fields, turbulence and gravity indicate that gravity dominates the dynamical state of G11, but with significant contribution from magnetic fields. The field strength, $|\mathbf{B}|$, increases slower than the gas density, n, from the envelope to the spine of G11, characterized by $|\mathbf{B}| \propto n^{0.3}$. The observed strength and orientation of magnetic fields in G11 imply that supersonic and sub-Alfvénic gas flow is channelled by the strong magnetic fields and is assembled into filaments perpendicular to the magnetic fields. The formation of low-mass stars is enhanced in the filaments with high column density, in agreement with the excess of low-mass protostars detected in the densest regions of G11.

17. A Parsec-Scale Catalog of Molecular Clouds in the Solar Neighborhood Based on 3D Dust Mapping: Implications for the Mass-Size Relation

Shlomo Cahlon, Catherine Zucker, Alyssa Goodman, Charles Lada, João Alves ★ We dendrogram the Leike et al. 2020 3D dust map, leveraging its ~ 1 pc spatial resolution to produce a uniform catalog of molecular clouds in the solar neighborhood. Using accurate distances, we measure the properties of 65 clouds in true 3D space, eliminating much of the uncertainty in mass, size, and density. Clouds in the catalog contain a total of 1.1×10^5 $M_\odot$, span distances of $116 - 440$ pc, and include a dozen well-studied clouds in the literature. In addition to deriving cloud properties in 3D volume density space, we create 2D dust extinction maps from the 3D data by projecting the 3D clouds onto a 2D "Sky" view. We measure the properties of the 2D clouds separately from those of the 3D clouds. Using the 2D and 3D derived results, we compare the scaling relation between the masses and sizes of clouds following Larson 1981. We find that our 2D projected mass-size relation, $M \propto r^{2.1}$, agrees with Larson's Third Relation, but our 3D derived properties lead to a scaling relation of about one order larger: $M \propto r^{2.9}$. Validating predictions from numerical simulations and analytic theory, our results indicate that the mass-size relation is sensitive to whether column or volume density is used to define clouds, since mass scales with area in 2D space ($M \propto r^2$) and with volume in 3D space ($M \propto r^3$). Our results imply a roughly constant column and volume density for molecular clouds, as would be expected for clouds where the lower density, larger volume-filling gas dominates the cloud mass budget.

18. On the survivability of a population of gas giant planets on wide orbits

Ethan Carter, Dimitris Stamatellos ★ The existence of giant planets on wide orbits ($\gtrsim$ 100AU) challenge planet formation theories; the core accretion scenario has difficulty in forming them, whereas the disc instability model forms an overabundance of them that is not seen observations. We perform N-body simulations investigating the effect of close stellar encounters ($\leq$ 1200AU) on systems hosting wide-orbit giant planets and the extent at which such interactions may disrupt the initial wide-orbit planet population. We find that the effect of an interaction on the orbit of a planet is stronger for high-mass, low-velocity perturbers, as expected. We find that due to just a single encounter there is a $\sim 17\%$ chance that the wide-orbit giant planet is liberated in the field, a $\sim 10\%$ chance it is scattered significantly outwards, and a $\sim 6\%$ chance it is significantly scattered inwards. Moreover, there is a $\sim 21\%$ chance that its eccentricity is excited to e>0.1, making it more prone to disruption in subsequent encounters. The results strongly suggest that the effect of even a single stellar encounter is significant in disrupting the primordial wide-orbit giant planet population; in reality the effect will be even more prominent, as in a young star-forming region more such interactions are expected to occur. We conclude that the low occurrence rate of wide-orbit planets revealed by observational surveys does not exclude the possibility that such planetary systems are initially abundant, and therefore the disc-instability model may be a plausible scenario for their formation.

19. The diverse chemistry of protoplanetary disks as revealed by JWST

Ewine F. van Dishoeck, S. Grant, B. Tabone, M. van Gelder, L. Francis, L. Tychoniec, G. Bettoni, A. M. Arabhavi, D. Gasman, P. Nazari, M. Vlasblom, P. Kavanagh, V. Christiaens, P. Klaassen, H. Beuther, Th. Henning, I. Kamp ★ Early results from the JWST-MIRI guaranteed time programs on protostars (JOYS) and disks (MINDS) are presented. Thanks to the increased sensitivity, spectral and spatial resolution of the MIRI spectrometer, the chemical inventory of the planet-forming zones in disks can be investigated with unprecedented detail across stellar mass range and age. Here data are presented for five disks, four around low-mass stars and one around a very young high-mass star. The mid-infrared spectra show some similarities but also significant diversity: some sources are rich in CO2, others in H2O or C2H2. In one disk around a very low-mass star, booming C2H2 emission provides evidence for a "soot" line at which carbon grains are eroded and sublimated, leading to a rich hydrocarbon chemistry in which even di-acetylene (C4H2) and benzene (C6H6) are detected (Tabone et al. 2023). Together, the data point to an active inner disk gas-phase chemistry that is closely linked to the physical structure (temperature, snowlines, presence of cavities and dust traps) of the entire disk and which may result in varying CO2/H2O abundances and high C/O ratios >1 in some cases. Ultimately, this diversity in disk chemistry will also be reflected in the diversity of the chemical composition of exoplanets.

20. 3-D SPH simulations of the FUOR flares in the clumpy accretion model

Tatiana V. Demidova, Vladimir P. Grinin ★ One of the early hypotheses about the origin of FUOR outbursts explains them by the fall of gas clumps from the remnants of protostellar clouds onto protoplanetary disks surrounding young stars (Hartmann and Kenyon 1985). To calculate the consequences of such an event we make 3D hydrodynamic simulations by SPH method. It is shown that the fall of the clump on the disk in the vicinity of the star actually causes a burst of the star's accretion activity, resembling in its characteristics the flares of known FUORs. In the region of incidence, an inhomogeneous gas ring is formed, which is inclined relative to the outer disk. During several revolutions around the star, this ring combines with the inner disk and forms a tilted disk. In the process of evolution, the inner disk expands, and its inclination relative to the outer disk decreases. After 100 revolutions, the angle of inclination is a few degrees. This result is of interest in connection with the discovery in recent years of protoplanetary disks, the inner region of which is inclined relative to the outer one. Such structures are usually associated with the existence in the vicinity of a star of a massive body (planet or brown dwarf), whose orbit is inclined relative to the plane of the disk. The results of our modeling indicate the possibility of an alternative explanation for this phenomenon.

21. Constraints on the dust size distributions in the HD 163296 disk from the difference of the apparent dust ring widths between two ALMA Bands

Kiyoaki Doi, Akimasa Kataoka ★ The dust size in protoplanetary disks is a crucial parameter for understanding planet formation, while the observational constraints on dust size distribution have large uncertainties. In this study, we present a new method to constrain the dust size distribution from the dust spatial distribution, utilizing the fact that larger dust grains are more spatially localized. We analyze the ALMA Band 6 (1.25 mm) and Band 4 (2.14 mm) high-resolution images and constrain the dust size distribution in the two rings of the HD 163296 disk. We find that the outer ring at 100 au appears narrower at the longer wavelengths, while the inner ring at 67 au appears to have similar widths across the two wavelengths. We model dust rings trapped at gas pressure maxima, where the dust grains follow a power-law size distribution, and the dust grains of a specific size follow a Gaussian spatial distribution with the width depending on the grain size. By comparing the observations with the models, we constrain the maximum dust size $a_{\max}$ and the exponent of the dust size distribution p. We constrain that 0.9 mm $< a_{\max} < 5$ mm and $p < 3.3$ in the inner ring, and $a_{\max} > 3 \times 10^1$ mm and $3.4 < p < 3.7$ in the outer ring. The larger maximum dust size in the outer ring implies a spatial dependency in dust growth, potentially influencing the formation location of the planetesimals. We further discuss the turbulence strength α derived from the constrained dust spatial distribution, assuming equilibrium between turbulent diffusion and accumulation of dust grains.

22. Lowest accreting protoplanetary discs consistent with X-ray photoevaporation driving their final dispersal

Barbara Ercolano, Giovanni Picogna, Kristina Monsch ★ Photoevaporation from high energy stellar radiation has been thought to drive the dispersal of protoplanetary discs. Different theoretical models have been proposed, but their predictions diverge in terms of the rate and modality at which discs lose their mass, with significant implications for the formation and evolution of planets. In this paper we use disc population synthesis models to interpret recent observations of the lowest accreting protoplanetary discs, comparing predictions from EUV-driven, FUV-driven and X-ray driven photoevaporation models. We show that the recent observational data of stars with low accretion rates (low accretors) point to X-ray photoevaporation as the preferred mechanism driving the final stages of protoplanetary disc dispersal. We also show that the distribution of accretion rates predicted by the X-ray photoevaporation model is consistent with observations, while other dispersal models tested here are clearly ruled out.

23. Parsec scales of carbon chain and complex organic molecules in AFGL 2591 and IRAS 20126

P. Freeman, S. Bottinelli, R. Plume, E. Caux, C. Monaghan, B. Mookerjea ★ (Abridged) There is a diverse chemical inventory in protostellar regions leading to the classification of extreme types of systems. Warm carbon chain chemistry sources, for one, are the warm and dense regions near a protostar containing unsaturated carbon chain molecules. Since the presentation of this definition in 2008, there is a growing field to detect and characterise these sources. The details are lesser known in relation to hot cores and in high-mass star-forming regions – regions of great importance in galactic evolution. To investigate the prevalence of carbon chain species and their environment in high-mass star-forming regions, we have conducted targeted spectral surveys of two sources in the direction of Cygnus X – AFGL 2591 and IRAS 20126+4104 – with the Green Bank Telescope and the IRAM 30m Telescope. We have constructed a Local Thermodynamic Equilibrium (LTE) model using the observed molecular spectra to determine the physical environment in which these molecules originate. We map both the observed spatial distribution and the physical parameters found from the LTE model. We also determine the formation routes of these molecules in each source using the three-phase NAUTILUS chemical evolution code. We detect several lines of propyne, CH_3CCH, and cyclopropenylidene, c-C_3H_2 as tracers of carbon chain chemistry, as well as several lines of formaldehyde, H_2CO, and methanol, CH_3OH, as a precursor and a tracer of complex organic molecule chemistry, respectively. We find excitation temperatures of 20-30 K for the carbon chains and 8-85 K for the complex organics. The CH_3CCH abundances are reproduced by a warm-up model, consistent with warm carbon chain chemistry, while the observed CH_3OH abundances require a shock mechanism sputtering the molecules into the gas phase.

24. γ-ray detection from occasional flares in T Tauri stars of NGC 2071. I. Observational connection

A. Filócomo, J. F. Albacete Colombo, E. Mestre, L. J. Pellizza, J. A. Combi ★ NGC 2071 is a star-forming region that overlaps with three γ-ray sources detected by the Fermi Space Telescope. We propose that strong flare activity in T Tauri stars could produce γ-ray emission in a way that makes them a counterpart to some unidentified sources detected by the Large Area Telescope aboard the Fermi satellite. We have performed a spectral and temporal analysis for two Fermi data sets: the first 2 yr and the entire 14 yr of observations. We have found that the γ-ray source is detectable at 3.2σ above the background at energies above 100 GeV during the first 2 yr of observation. The analysis of the expected frequency of the highest energy flares occurring in T Tauri stars is consistent with our estimate. In addition, we have determined the minimum energy of the flare that would produce γ-ray emission, which is $\sim 5 \times 10^{37}$ erg. This agreement becomes a hard observational constraint supporting previous hypotheses about rare flares as the origin of unidentified γ-ray sources in star-forming regions.

25. Modelling UX Ori Star Eclipses based on Spectral Observations with the Nordic Optical Telescope. I. RR Tau

V. P. Grinin, L. V. Tambovtseva, A. A. Djupvik, G. Gahm, T. Grenman, H. Weber, H. Bengtsson, H. De Angelis, G. Duszanowicz, D. Heinonen, G. Holmberg, T. Karlsson, M. Larsson, J. Warell, T. Wikander ★ Based on observations obtained with the Nordic Optical Telescope we investigate the spectral variability of the Herbig Ae star RR Tau. This star belongs to the UX Ori family, characterized by very deep fadings caused by the screening of the star with opaque fragments (clouds) of the protoplanetary discs. At the moments of such minima one observes strong spectral variability due to the fact that the dust cloud occults, for an observer, not only the star but also a part of the region where the emission spectrum originates. We calculated a series of obscuration models to interpret the observed variability of the H-alpha line parameters. We consider two main obscuration scenarios: (1) the dust screen rises vertically above the circumstellar disc, and (2) the screen intersects the line-of-sight moving azimuthally with the disc. In both cases the model of the emission region consists of a compact magnetosphere and a magneto-centrifugal disc wind. Comparison with observations shows that the first scenario explains well the variability of the radiation flux, the equivalent width, as well as the asymmetry of the H-alpha line during eclipses, while the second scenario explains them only partly. This permits us to suggest that in the case of RR Tau, the main causes of the eclipses are either a structured disc wind, or the charged dust lifted along the field lines of the poloidal component of the magnetic field of the circumstellar disc.

26. Multiples among B stars in the Scorpius-Centaurus association

R. Gratton, V. Squicciarini, V. Nascimbeni, M. Janson, S. Reffert, M. Meyer, P. Delorme, E. E. Mamajek, M. Bonavita, S. Desidera, D. Mesa, E. Rigliaco, V. D'Orazi, C. Lazzoni, G. Chauvin, M. Langlois ★ We discuss the properties of companions to B stars in the Scorpius-Centaurus association (age 15 Myr, 181 B-stars). We gathered available data combining high contrast imaging samples with evidence of companions from Gaia, from eclipsing binaries, and from spectroscopy. We evaluated the completeness of the binary search and estimated the mass and semi-major axis for all detected companions. These data provide a complete sample of stellar secondaries for separation >3 au, and they are highly informative as to closer companions. We found evidence for 200 companions around 181 stars. The fraction of single star is $15.2 \pm 4.1\%$ for stars with M_A3.5 Msun while it is $31.5\pm$ 5.9% for lower-mass stars. The median semi-major axis of the orbits of the companions is smaller for B than in A stars, confirming a turn-over previously found for OB stars. The mass distribution of the very wide (a>1000 au) and closer companions is different. Very few companions of massive stars M_A >5.0 Msun have a mass below solar and even fewer are M stars with a semi-major axis <1000 au. The scarcity of low-mass companions extends throughout the whole sample. Most early B stars are in compact systems with massive secondaries, while lower-mass stars are mainly in wider systems with a larger spread in mass ratios. We interpret our results as the formation of secondaries with a semi-major axis <1000 au (about 80% of the total) by fragmentation of the disk of the primary and selective mass accretion on the secondaries. The observed trends with primary mass may be explained by a more prolonged phase of accretion episodes on the disk and by a more effective inward migration. We detected twelve new stellar companions from the BEAST survey and of a new BD companion at 9.6 arcsec from HIP74752 using Gaia data, and we discuss the cases of possible BD and low-mass stellar companions to HIP59173, HIP62058, and HIP64053.

27. The $\dot{M}$–$M_{\rm disk}$ relationship for Herbig Ae/Be stars: a lifetime problem for disks with low masses?

Sierra L. Grant, Lucas M. Stapper, Michiel R. Hogerheijde, Ewine F. van Dishoeck, Sean Brittain, Miguel Vioque ★ The accretion of material from protoplanetary disks onto their central stars is a fundamental process in the evolution of these systems and a key diagnostic in constraining the disk lifetime. We analyze the relationship between the stellar accretion rate and the disk mass in 32 intermediate-mass Herbig Ae/Be systems and compare them to their lower-mass counterparts, T Tauri stars. We find that the $\dot{M}$–$M_{\rm disk}$ relationship for Herbig Ae/Be stars is largely flat at $\sim10^{-7}$ $M_\odot$ yr^{-1} across over three orders of magnitude in dust mass. While most of the sample follows the T Tauri trend, a subset of objects with high accretion rates and low dust masses are identified. These outliers (12 out of 32 sources) have an inferred disk lifetime of less than 0.01 Myr and are dominated by objects with low infrared excess. This outlier sample is likely identified in part by the bias in classifying Herbig Ae/Be stars, which requires evidence of accretion that can only be reliably measured above a rate of $\sim10^{-9}$ $M_\odot$ yr^{-1} for these spectral types. If the disk masses are not underestimated and the accretion rates are not overestimated, this implies that these disks may be on the verge of dispersal, which may be due to efficient radial drift of material or outer disk depletion by photoevaporation and/or truncation by companions. This outlier sample likely represents a small subset of the larger young, intermediate-mass stellar population, the majority of which would have already stopped accreting and cleared their disks.

28. ALMA Survey of Orion Planck Galactic Cold Clumps (ALMASOP): The Warm-Envelope Origin of Hot Corinos

Shih-Ying Hsu, Sheng-Yuan Liu, Doug Johnstone, Tie Liu, Leonardo Bronfman, Huei-Ru Vivien Chen, Somnath Dutta, David J. Eden, Neal J. Evans II, Naomi Hirano, Mika Juvela, Yi-Jehng Kuan, Woojin Kwon, Chin-Fei Lee, Chang Won Lee, Jeong-Eun Lee, Shanghuo Li, Chun-Fan Liu, Xunchuan Liu, Qiuyi Luo, Sheng-Li Qin, Mark G. Rawlings, Dipen Sahu, Patricio Sanhueza, Hsien Shang, Kenichi Tatematsu, Yao-Lun Yang ★ Hot corinos are of great interest due to their richness in interstellar complex organic molecules (COMs) and the consequent potential prebiotic connection to solar-like planetary systems. Recent surveys have reported an increasing number of hot corino detections in Class 0/I protostars; however, the relationships between their physical properties and the hot-corino signatures remain elusive. In this study, our objective is to establish a general picture of the detectability of the hot corinos by identifying the origin of the hot-corino signatures in the sample of young stellar objects (YSOs) obtained from the Atacama Large Millimeter/submillimeter Array Survey of Orion Planck Galactic Cold Clumps (ALMASOP) project. We apply spectral energy distribution (SED) modeling to our sample and identify the physical parameters of the modeled YSOs directly, linking the detection of hot-corino signatures to the envelope properties of the YSOs. Imaging simulations of the methanol emission further support this scenario. We, therefore, posit that the observed COM emission originates from the warm inner envelopes of the sample YSOs, based on both the warm region size and the envelope density profile. The former is governed by the source luminosity and is additionally affected by the disk and cavity properties, while the latter is related to the evolutionary stages. This scenario provides a framework for detecting hot-corino signatures toward luminous Class 0 YSOs, with fewer detections observed toward similarly luminous Class I sources.

29. Forming rocky exoplanets around K-dwarf stars

P. Hatalova, R. Brasser, E. Mamonova, S. C. Werner ★ How multiple close-in super-Earths form around stars with masses lower than that of the Sun is still an open issue. Several recent modeling studies have focused on planet formation around M-dwarf stars, but so far no studies have focused specifically on K dwarfs, which are of particular interest in the search for extraterrestrial life. We aim to reproduce the currently known population of close-in super-Earths observed around K-dwarf stars and their system characteristics. We performed 48 high-resolution N-body simulations of planet formation via planetesimal accretion using the existing GENGA software running on GPUs. In the simulations we varied the initial disk mass and the solid and gas surface density profiles. Each simulation began with 12000 bodies with radii of between 200 and 2000 km around two different stars, with masses of 0.6 and 0.8 $M_\odot$. Most simulations ran for 20 Myr, with several simulations extended to 40 or 100 Myr. The mass distributions for the planets with masses between 2 and 12 $M_\oplus$ show a strong preference for planets with masses $M_p < 6$ $M_\oplus$ and a lesser preference for planets with larger masses, whereas the mass distribution for the observed sample increases almost linearly. However, we managed to reproduce the main characteristics and architectures of the known planetary systems and produce mostly long-term angular-momentum-deficit-stable, nonresonant systems, but we require an initial disk mass of 15 $M_\oplus$ or higher and a gas surface density value at 1 AU of 1500 g cm^{-2} or higher. Our simulations also produce many low-mass planets with $M < 2$ $M_\oplus$, which are not yet found in the observed population, probably due to the observational biases. The final systems contain only a small number of planets, which could possibly accrete substantial amounts of gas, and these formed after the gas had mostly dissipated.

30. The VLT MUSE NFM view of outflows and externally photoevaporating discs near the Orion Bar

Thomas J. Haworth, Megan Reiter, C. Robert O'Dell, Peter Zeidler, Olivier Berne, Carlo F. Manara, Giulia Ballabio, Jinyoung S. Kim, John Bally, Javier R. Goicoechea, Mari-Liis Aru, Aashish Gupta, Anna Miotello ★ We present VLT/MUSE Narrow Field Mode (NFM) observations of a pair of disc-bearing young stellar objects towards the Orion Bar: 203-504 and 203-506. Both of these discs are subject to external photoevaporation, where winds are launched from their outer regions due to environmental irradiation. Intriguingly, despite having projected separation from one another of only 1.65 arcsec (660au at 400pc), 203-504 has a classic teardrop shaped "proplyd" morphology pointing towards θ^2Ori A (indicating irradiation by the EUV of that star, rather than θ^1 Ori C) but 203-506 has no ionisation front, indicating it is not irradiated by stellar EUV at all. However, 203-506 does show [CI] 8727Å and [OI] 6300Å in emission, indicating irradiation by stellar FUV. This explicitly demonstrates the importance of FUV irradiation in driving mass loss from discs. We conclude that shielding of 203-506 from EUV is most likely due to its position on the observers side of an ionized layer lying in the foreground of the Huygens Region. We demonstrate that the outflow HH 519, previously thought to be emanating from 203-504 is actually an irradiated cloud edge and identify a new compact outflow from that object approximately along our line of sight with a velocity $\sim 130\,\mathrm{km\,s^{-1}}$.

31. Twenty-Five Years of Accretion onto the Classical T Tauri Star TW Hya

Gregory J. Herczeg, Yuguang Chen, Jean-Francois Donati, Andrea K. Dupree, Frederick M. Walter, Lynne A. Hillenbrand, Christopher M. Johns-Krull, Carlo F. Manara, Hans Moritz Guenther, Min Fang, P. Christian Schneider, Jeff A. Valenti, Silvia H. P. Alencar, Laura Venuti, Juan Manuel Alcala, Antonio Frasca, Nicole Arulanantham, Jeffrey L. Linsky, Jerome Bouvier, Nancy S. Brickhouse, Nuria Calvet, Catherine C. Espaillat, Justyn Campbell-White, John M. Carpenter, Seok-Jun Chang, Kelle L. Cruz, S. E. Dahm, Jochen Eisloeffel, Suzan Edwards, William J. Fischer, Zhen Guo, Thomas Henning, Tao Ji, Jesse Jose, Joel H. Kastner, Ralf Launhardt, David A. Principe, Conner E. Robinson, Javier Serna, Michal Siwak, Michael F. Sterzik, Shinsuke Takasao ★ Accretion plays a central role in the physics that governs the evolution and dispersal of protoplanetary disks. The primary goal of this paper is to analyze the stability over time of the mass accretion rate onto TW Hya, the nearest accreting solar-mass young star. We measure veiling across the optical spectrum in 1169 archival high-resolution spectra of TW Hya, obtained from 1998–2022. The veiling is then converted to accretion rate using 26 flux-calibrated spectra that cover the Balmer jump. The accretion rate measured from the excess continuum has an average of 2.51×10^{-9} $M_\odot$ yr^{-1} and a Gaussian distribution with a FWHM of 0.22 dex. This accretion rate may be underestimated by a factor of up to 1.5 because of uncertainty in the bolometric correction and another factor of 1.7 because of excluding the fraction of accretion energy that escapes in lines, especially Lyα. The accretion luminosities are well correlated with He line luminosities but poorly correlated with Hα and Hβ luminosity. The accretion rate is always flickering over hours but on longer timescales has been stable over 25 years. This level of variability is consistent with previous measurements for most, but not all, accreting young stars.

32. Filament fragmentation: Density gradients suppress end dominated collapse

Elena Hoemann, Stefan Heigl, Andreas Burkert ★ The onset of star formation is set by the collapse of filaments in the interstellar medium. From a theoretical point of view, an isolated cylindrical filament forms cores via the edge effect. Due to the self-gravity of a filament, the strong increase in acceleration at both ends leads to a pile-up of matter which collapses into cores. However, this effect is rarely observed. Most theoretical models consider a sharp density cut-off at the edge of the filament, whereas a smoother transition is more realistic and would also decrease the acceleration at the ends of the filament. We show that the edge effect can be significantly slowed down by a density gradient, although not completely avoided. However, this allows perturbations inside the filament to grow faster than the edge. We determine the critical density gradient for which the timescales are equal and find it to be of the order of several times the filament radius. Hence, the density gradient at the ends of a filament is an essential parameter for fragmentation and the low rate of observed cases of the edge effect could be naturally explained by shallow gradients.

33. Measuring the Numerical Viscosity in Simulations of Protoplanetary Disks in Cartesian Grids – The Viscously Spreading Ring Revisited

Jibin Joseph, Alexandros Ziampras, Lucas Jordan, George A. Turpin, Richard P. Nelson ★ Hydrodynamical simulations solve the governing equations on a discrete grid of space and time. This discretization causes numerical diffusion similar to a physical viscous diffusion, whose magnitude is often unknown or poorly constrained. With the current trend of simulating accretion disks with no or very low prescribed physical viscosity, it becomes essential to understand and quantify this inherent numerical diffusion, in the form of a numerical viscosity. We study the behavior of the viscous spreading ring and the spiral instability that develops in it. We then use this setup to quantify the numerical viscosity in Cartesian grids and study its properties. We simulate the viscous spreading ring and the related instability on a two-dimensional polar grid using PLUTO as well as FARGO, and ensure convergence of our results with a resolution study. We then repeat our models on a Cartesian grid and measure the numerical viscosity by comparing results to the known analytical solution, using PLUTO and Athena++. We find that the numerical viscosity in a Cartesian grid scales with resolution as approximately $\nu_{num} \propto \Delta x^2$ and is equivalent to an effective $\alpha \sim 10^{-4}$ for a common numerical setup. We also show that the spiral instability manifests as a single leading spiral throughout the whole domain on polar grids. This is contrary to previous results and indicates that sufficient resolution is necessary in order to correctly resolve the instability. Our results are relevant in the context of models where the origin should be included in the computational domain, or when polar grids cannot be used. Examples of such cases include models of disk accretion onto a central binary and inherently Cartesian codes.

34. N-body simulation of planetary formation through pebble accretion in a radially structured protoplanetary disk

Tenri Jinno, Takayuki R. Saitoh, Yota Ishigaki, Junichiro Makino ★ In the conventional theory of planet formation, it is assumed that protoplanetary disks are axisymmetric and have a smooth radial profile. However, recent radio observations of protoplanetary disks have revealed that many of them have complex radial structures. In this study, we perform a series of N-body simulations to investigate how planets are formed in protoplanetary disks with radial structures. For this purpose, we consider the effect of continuous pebble accretion onto the discontinuity boundary within the terrestrial planet-forming region (~ 0.6 AU). We found that protoplanets grow efficiently at the discontinuity boundary, reaching the Earth mass within $\sim 10^4$ years. We confirmed that giant collisions of protoplanets occur universally in our model. Moreover, we found that multiple planet-sized bodies form at regular intervals in the vicinity of the discontinuity boundary. These results indicate the possibility of the formation of solar system-like planetary systems in radially structured protoplanetary disks.

35. Unveiling the Dynamics of Dense Cores in Cluster-Forming Clumps: A 3D MHD Simulation Study of Angular Momentum and Magnetic Field Properties

Shinichi. W. Kinoshita, Fumitaka Nakamura ★ We conducted isothermal MHD simulations with self-gravity to investigate the properties of dense cores in cluster-forming clumps. Two different setups were explored: a single rotating clump and colliding clumps. We focused on determining the extent to which the formed dense cores inherit the rotation and magnetic field of the parental clump. Our statistical analysis revealed that the alignment between the angular momentum of dense cores, $\mathbf{L}_{\rm core}$, and the rotational axis of the clump is influenced by the strength of turbulence and the simulation setup. In single rotating clumps, we found that $\mathbf{L}_{\rm core}$ tends to align with the clump's rotational axis if the initial turbulence is weak. However, in colliding clumps, this alignment does not occur, regardless of the initial turbulence strength. This misalignment in colliding clumps is due to the induced turbulence from the collision and the isotropic gas inflow into dense cores. Our analysis of colliding clumps also revealed that the magnetic field globally bends along the shock-compressed layer, and the mean magnetic field of dense cores, $\mathbf{B}_{\rm core}$, aligns with it. Both in single rotating clumps and colliding clumps, we found that the angle between $\mathbf{B}_{\rm core}$ and $\mathbf{L}_{\rm core}$ is generally random, regardless of the clump properties. We also analyzed the dynamical states of the formed cores and found a higher proportion of unbound cores in colliding clumps. In addition, the contribution of rotational energy was only approximately 5% of the gravitational energy, regardless of the model parameters for both single and colliding cases.

36. Kinematic signatures of a low-mass planet with a moderately inclined orbit in a protoplanetary disk

Kazuhiro D. Kanagawa, Tomohiro Ono, Munetake Momose ★ A planet embedded in a protoplanetary disk produces a gap by disk-planet interaction. It also generates velocity perturbation of gas, which can also be observed as deviations from the Keplerian rotation in the channel map of molecular line emission, called kinematic planetary features. These observed signatures provide clues to determine the mass of the planet. We investigated the features induced by the planet with an inclined orbit through three-dimensional hydrodynamic simulations. We found that a smaller planet, with the inclination being $\sim 10^\circ$ – 20°, can produce kinematic features as prominent as those induced by the massive coplanar planet. Despite the kinematic features being similar, the gap is shallower and narrower as compared with the case in which the kinematic features are formed by the coplanar planet. We also found that the kinematic features induced by the inclined planet were fainter for rarer CO isotopologues because the velocity perturbation is weaker at the position closer to the midplane, which was different in the case with a coplanar massive planet. This dependence on the isotopologues is distinguished if the planet has the inclined orbit. We discussed two observed kinematic features in the disk of HD 163296. We concluded that the kink observed at 220 au can be induced by the inclined planet, while the kink at 67 au is consistent to that induced by the coplanar planet.

37. Modelling Star Cluster Formation: Gas Accretion

Jeremy Karam, Alison Sills ★ The formation of star clusters involves the growth of smaller, gas-rich subclusters through accretion of gas from the giant molecular cloud within which the subclusters are embedded. The two main accretion mechanisms responsible for this are accretion of gas from dense filaments, and from the ambient background of the cloud. We perform simulations of both of these accretion processes onto gas-rich star clusters using coupled smoothed particle hydrodynamics to model the gas, and N-body dynamics to model the stars. We find that, for both accretion processes, the accreting star cluster loses some of its original mass while gaining mass from either the ambient background or the dense filament. The amount of mass lost from both these processes is small compared to the total mass of the cluster. However, in the case of accretion from a background medium, the net effect can be a decrease in the total mass of the cluster if it is travelling fast enough through the ambient medium (> 4kms^{-1}). We find that the amount of mass lost from the cluster through filamentary accretion is independent of the density, width, or number of filaments funneling gas into the cluster and is always such that the mass of the cluster is constantly increasing with time. We compare our results to idealized prescriptions used to model star cluster formation in larger scale GMC simulations and find that such prescriptions act as an upper limit when describing the mass of the star cluster they represent.

38. Initial conditions of star formation at $\lesssim$2000 au: physical structure and NH_3 depletion of three early-stage cores

Yuxin Lin, Silvia Spezzano, Jaime E. Pineda, Jorma Harju, Anika Schmiedeke, Sihan Jiao, Hauyu Baobab Liu, Paola Caselli ★ Pre-stellar cores represent a critical evolutionary phase in low-mass star formation. We aim to unveil the detailed thermal structure and density distribution of three early-stage cores, starless core L1517B, and prestellar core L694-2 and L429, with the high angular resolution observations of the NH_3 (1,1) and (2,2) inversion transitions obtained with VLA and GBT. In addition, we explore where/if NH_3 depletes in the central regions. Applying the mid-infrared extinction method to the *Spitzer* 8 μm map we obtain a high angular resolution hydrogen column density map, and derive the gas density profile to assess the variation of NH_3 abundance as a function of gas volume density. The measured temperature profiles of L429 and L1517B show a minor decrease towards the core center, dropping from $\sim$9$\tilde{K}$ to below 8$\tilde{K}$, and $\sim$11 K to 10 K, while L694-2 has a rather uniform temperature distribution around $\sim$9 K. Among the three cores, L429 has the highest central gas density, close to sonic velocity line-width, and largest localised velocity gradient, all indicative of an advanced evolutionary stage. We resolve that the abundance of NH_3 becomes two times lower in the central region of L429, occurring around a gas density of 4.4×10^4 cm^{-3}. Compared to Ophiuchus/H-MM1 which shows an even stronger drop of the NH_3 abundance at 2×10^5 cm^{-3}, the abundance variations of the three cores plus Ophiuchus/H-MM1 suggest a progressive NH_3 depletion with increasing central density of the core.

39. The Dusty Rossby Wave Instability (DRWI): Linear Analysis and Simulations of Turbulent Dust-Trapping Rings in Protoplanetary Discs

Hanpu Liu, Xue-Ning Bai ★ Recent numerical simulations have revealed that dust clumping and planetesimal formation likely proceed in ring-like disc substructures, where dust gets trapped in weakly turbulent pressure maxima. The streaming instability has difficulty operating in such rings with external turbulence and no pressure gradient. To explore potential paths to planetesimal formation in this context, we analyse the stability of turbulent dust-trapping ring under the shearing sheet framework. We self-consistently establish the pressure maximum and the dust ring in equilibrium, the former via a balance of external forcing versus viscosity and the latter via dust drift versus turbulent diffusion. We find two types of $\gtrsim H$-scale instabilities (H being the pressure scale height), which we term the dusty Rossby wave instability (DRWI). Type I is generalised from the standard RWI, which is stationary at the pressure maximum and dominates in relatively sharp pressure bumps. Type II is a newly identified travelling mode that requires the presence of dust. It can operate in relatively mild bumps, including many that are stable to the standard RWI, and its growth rate is largely determined by the equilibrium gas and dust density gradients. We further conduct two-fluid simulations that verify the two types of the DRWI. While Type I leads strong to dust concentration into a large gas vortex similar to the standard RWI, the dust ring is preserved in Type II, and meanwhile exhibiting additional clumping within the ring. The DRWI suggests a promising path towards formation of planetesimals/planetary embryos and azimuthally asymmetric dust structure from turbulent dust-trapping rings.

40. Triple spiral arms of a triple protostar system imaged in molecular lines

Jeong-Eun Lee, Tomoaki Matsumoto, Hyun-Jeong Kim, Seokho Lee, Daniel Harsono, Jaehan Bae, Neal J. Evans II, Shu-ichiro Inutsuka, Minho Choi, Ken'ichi Tatematsu, Jae-Joon Lee, Dan Jaffe ★ Most stars form in multiple star systems. For a better understanding of their formation processes, it is important to resolve the individual protostellar components and the surrounding envelope and disk material at the earliest possible formation epoch because the formation history can be lost in a few orbital timescales. Here we present the ALMA observational results of a young multiple protostellar system, IRAS 04239+2436, where three well-developed large spiral arms were detected in the shocked SO emission. Along the most conspicuous arm, the accretion streamer was also detected in the SO_2 emission. The observational results are complemented by numerical magneto-hydrodynamic simulations, where those large arms only appear in magnetically weakened clouds. The numerical simulations also suggest that the large triple spiral arms are the result of gravitational interactions between compact triple protostars and the turbulent infalling envelope.

41. Complex Organic Molecules in a Very Young Hot Corino, HOPS 373SW

Jeong-Eun Lee, Giseon Baek, Seokho Lee, Jae-Hong Jeong, Chul-Hwan Kim, Yuri Aikawa, Gregory J. Herczeg, Doug Johnstone, John J. Tobin ★ We present the spectra of Complex Organic Molecules (COMs) detected in HOPS 373SW with the Atacama Large Millimeter/submillimeter Array (ALMA). HOPS 373SW, which is a component of a protostellar binary with a separation of 1500 au, has been discovered as a variable protostar by the JCMT Transient monitoring survey with a modest 30% brightness increase at submillimeter wavelengths. Our ALMA Target of Opportunity (ToO) observation at 345 GHz for HOPS 373SW revealed extremely young chemical characteristics with strong deuteration of methanol. The dust continuum opacity is very high toward the source center, obscuring line emission from within 0.03 arcsec. The other binary component, HOPS 373NE, was detected only in C17O in our observation, implying a cold and quiescent environment. We compare the COMs abundances relative to CH3OH in HOPS 373SW with those of V883 Ori, which is an eruptive disk object, as well as other hot corinos, to demonstrate the chemical evolution from envelope to disk. High abundances of singly, doubly, and triply deuterated methanol (CH2DOH, CHD2OH, and CD3OH) and a low CH3CN abundance in HOPS 373SW compared to other hot corinos suggest a very early evolutionary stage of HOPS 373SW in the hot corino phase. Since the COMs detected in HOPS 373SW would have been sublimated very recently from grain surfaces, HOPS 373SW is a promising place to study the surface chemistry of COMs in the cold prestellar phase, before sublimation.

42. Brightness and mass accretion rate evolution during the 2022 burst of EX Lupi

F. Cruz-Sáenz de Miera, Á. Kóspál, P. Ábrahám, R. A. B. Claes, C. F. Manara, J. Wendeborn, E. Fiorellino, T. Giannini, B. Nisini, A. Sicilia-Aguilar, J. Campbell-White, J. M. Alcalá, A. Banzatti, Zs. M. Szabó, F. Lykou, S. Antoniucci, J. Varga, M. Siwak, S. Park, Zs. Nagy, M. Kun ★ EX Lupi is the prototype by which EXor-type outbursts were defined. It has experienced multiple accretion-related bursts and outbursts throughout the last decades, whose study have greatly extended our knowledge about the effects of these types of events. This star experienced a new burst in 2022. We used multi-band photometry to create color-color and color-magnitude diagrams to exclude the possibility that the brightening could be explained by a decrease in extinction. We obtained VLT/X-shooter spectra to determine the Lacc and Macc during the peak of the burst and after its return to quiescence using 2 methods: empirical relationships between line luminosity and Lacc, and a slab model of the whole spectrum. We examined the 130 year light curve of EX Lupi to provide statistics on the number of outbursts experienced during this period of time. Our analysis of the data taken during the 2022 burst confirmed that a change in extinction is not responsible for the brightening. Our two approaches in calculating the Macc were in agreement, and resulted in values that are 2 orders of magnitude above what had previously been estimated, thus suggesting that EX Lupi is a strong accretor even when in quiescence. We determined that in 2022 March the Macc increased by a factor of 7 with respect to the quiescent level. We also found hints that even though the Macc had returned to almost its pre-outburst levels, certain physical properties of the gas had not returned to the quiescent values. We found that the mass accreted during this three month event was 0.8 lunar masses, which is approximately half of what is accreted during a year of quiescence. We calculated that if EX Lupi remains as active as it has been for the past 130 years, during which it has experienced at least 3 outbursts and 10 bursts, then it will deplete the mass of its circumstellar material in less than 160000 yr.

43. Identification of the simplest sugar-like molecule glycolaldehyde towards the hot molecular core G358.93-0.03 MM1

Arijit Manna, Sabyasachi Pal, Serena Viti, Sekhar Sinha ★ Glycolaldehyde (CH_2OHCHO) is the simplest monosaccharide sugar in the interstellar medium, and it is directly involved in the origin of life via the 'RNA world' hypothesis. We present the first detection of glycolaldehyde (CH_2OHCHO) towards the hot molecular core G358.93-0.03 MM1 using the Atacama Large Millimeter/Submillimeter Array (ALMA). The calculated column density of CH_2OHCHO towards G358.93-0.03 MM1 is $(1.52\pm0.9)\times10^{16}$ cm^{-2} with an excitation temperature of 300 ± 68.5 K. The derived fractional abundance of CH_2OHCHO with respect to H_2 is $(4.90\pm2.92)\times10^{-9}$, which is consistent with that estimated by existing two-phase warm-up chemical models. We discuss the possible formation pathways of CH_2OHCHO within the context of hot molecular cores and hot corinos and find that CH_2OHCHO is likely formed via the reactions of radical HCO and radical CH_2OH on the grain surface of G358.93-0.03 MM1.

44. Star-disk interactions in the strongly accreting T Tauri Star S CrA N

H. Nowacki, E. Alecian, K. Perraut, B. Zaire, C. P. Folsom, K. Pouilly, J. Bouvier, R. Manick, G. Pantolmos, A. P. Sousa, C. Dougados, G. A. J. Hussain, S. H. P. Alencar, J. B. Le Bouquin ★ Aims : We aimed at constraining the accretion-ejection phenomena around the strongly-accreting Northern component of the S CrA young binary system (S CrA N) by deriving its magnetic field topology and its magnetospheric properties, and by detecting ejection signatures, if any. Methods : We led a two-week observing campaign on S CrA N with the ESPaDOnS optical spectropolarimeter at the Canada-France-Hawaii Telescope. We recorded 12 Stokes I and V spectra over 14 nights. We computed the corresponding Least-Square Deconvolution (LSD) profiles of the photospheric lines and performed Zeeman-Doppler Imaging (ZDI). We analysed the kinematics of noticeable emission lines, namely He I $\lambda5876$ and the four first lines of the Balmer series, known to trace the accretion process. Conclusions : The findings from spectropolarimetry are complementary to those provided by optical long-baseline interferometry, allowing us to construct a coherent view of the innermost regions of a young, strongly accreting star. Yet, the strong and complex magnetic field reconstructed for S CrA N is inconsistent with the observed magnetic signatures of the emission lines associated to the post-shock region. We recommend a multi-technique, synchronized campaign of several days to put more constrains on a system that varies on a ~ 1 day timescale.

45. On the importance of disc chemistry in the formation of protoplanetary disc rings

C. A. Nolan, B. Zhao, P. Caselli, Z. Y. Li ★ Radial substructures have now been observed in a wide range of protoplanetary discs (PPDs), from young to old systems, however their formation is still an area of vigorous debate. Recent magnetohydrodynamic (MHD) simulations have shown that rings and gaps can form naturally in PPDs when non-ideal MHD effects are included. However these simulations employ ad-hoc approximations to the magnitudes of the magnetic diffusivities in order to facilitate ring growth. We replace the parametrisation of these terms with a simple chemical network and grain distribution model to calculate the non-ideal effects in a more self-consistent way. We use a range of grain distributions to simulate grain formation for different disc conditions. Including ambipolar diffusion, we find that large grain populations ($> 1\mu$m), and those including a population of very small polyaromatic hydrocarbons (PAHs) facilitate the growth of periodic, stable rings, while intermediate sized grains suppress ring formation. Including Ohmic diffusion removes the positive influence of PAHs, with only large grain populations still producing periodic ring and gap structures. These results relate closely to the degree of coupling between the magnetic field and the neutral disc material, quantified by the non-dimensional Elsasser number Λ (the ratio of magnetic forces to Coriolis force). For both the ambipolar-only and ambipolar-ohmic cases, if the total Elsasser number is initially of order unity along the disc mid-plane, ring and gap structures may develop.

46. Planet formation throughout the Milky Way: Planet populations in the context of Galactic chemical evolution

Jesper Nielsen, Matthew Raymond Gent, Maria Bergemann, Philipp Eitner, Anders Johansen ★ As stellar compositions evolve over time in the Milky Way, so will the resulting planet populations. In order to place planet formation in the context of Galactic chemical evolution, we make use of a large ($N = 5\,325$) stellar sample representing the thin and thick discs, defined chemically, and the halo, and we simulate planet formation by pebble accretion around these stars. We build a chemical model of their protoplanetary discs, taking into account the relevant chemical transitions between vapour and refractory minerals, in order to track the resulting compositions of formed planets. We find that the masses of our synthetic planets increase on average with increasing stellar metallicity [Fe/H] and that giant planets and super-Earths are most common around thin-disc (α-poor) stars since these stars have an overall higher budget of solid particles. Giant planets are found to be very rare ($\lesssim$1%) around thick-disc (α-rich) stars and nearly non-existent around halo stars. This indicates that the planet population is more diverse for more metal-rich stars in the thin disc. Water-rich planets are less common around low-metallicity stars since their low metallicity prohibits efficient growth beyond the water ice line. If we allow water to oxidise iron in the protoplanetary disc, this results in decreasing core mass fractions with increasing [Fe/H]. Excluding iron oxidation from our condensation model instead results in higher core mass fractions, in better agreement with the core-mass fraction of Earth, that increase with increasing [Fe/H]. Our work demonstrates how the Galactic chemical evolution and stellar parameters, such as stellar mass and chemical composition, can shape the resulting planet population.

47. Dust enrichment and grain growth in a smooth disk around the DG Tau protostar revealed by ALMA triple bands frequency observations

Satoshi Ohashi, Munetake Momose, Akimasa Kataoka, Aya E Higuchi, Takashi Tsukagoshi, Takahiro Ueda, Claudio Codella, Linda Podio, Tomoyuki Hanawa, Nami Sakai, Hiroshi Kobayashi, Satoshi Okuzumi, Hidekazu Tanaka ★ Characterizing the physical properties of dust grains in a protoplanetary disk is critical to comprehending the planet formation process. Our study presents ALMA high-resolution observations of the young protoplanetary disk around DG Tau at a 1.3 mm dust continuum. The observations, with a spatial resolution of $\approx 0.04''$, or ≈ 5 au, revealed a geometrically thin and smooth disk without substantial substructures, suggesting that the disk retains the initial conditions of the planet formation. To further analyze the distributions of dust surface density, temperature, and grain size, we conducted a multi-band analysis with several dust models, incorporating ALMA archival data of the 0.87 mm and 3.1 mm dust polarization. The results showed that the Toomre Q parameter is $\lesssim 2$ at a 20 au radius, assuming a dust-to-gas mass ratio of 0.01. This implies that a higher dust-to-gas mass ratio is necessary to stabilize the disk. The grain sizes depend on the dust models, and for the DSHARP compact dust, they were found to be smaller than $\sim 400\ \mu$m in the inner region ($r \lesssim 20$ au), while exceeding larger than 3 mm in the outer part. Radiative transfer calculations show that the dust scale height is lower than at least one-third of the gas scale height. These distributions of dust enrichment, grain sizes, and weak turbulence strength may have significant implications for the formation of planetesimals through mechanisms such as streaming instability. We also discuss the CO snowline effect and collisional fragmentation in dust coagulation for the origin of the dust size distribution.

48. A dependence of binary and planetary system destruction on subtle variations in the substructure in young star-forming regions

Richard J. Parker ★ Simulations of the effects of stellar fly-bys on planetary systems in star-forming regions show a strong dependence on subtle variations in the initial spatial and kinematic substructure of the regions. For similar stellar densities, the more substructured star-forming regions disrupt up to a factor of two more planetary systems. We extend this work to look at the effects of substructure on stellar binary populations. We present N-body simulations of substructured, and non-substructured (smooth) star-forming regions in which we place different populations of stellar binaries. We find that for binary populations that are dominated by close (<100au) systems, a higher proportion are destroyed in substructured regions. However, for wider systems (>100au), a higher proportion are destroyed in smooth regions. The difference is likely due to the hard-soft, or fast-slow boundary for binary destruction. Hard (fast/close) binaries are more likely to be destroyed in environments with a small velocity dispersion (kinematically substructured regions), whereas soft (slow/wide) binaries are more likely to be destroyed in environments with higher velocity dispersions (non-kinematically substructured regions). Due to the vast range of stellar binary semimajor axes in star-forming regions ($10^{-2} - 10^{4}$au) these differences are small and hence unlikely to be observable. However, planetary systems have a much smaller initial semimajor axis range (likely ∼1 – 100au for gas giants) and here the difference in the fraction of companions due to substructure could be observed if the star-forming regions that disrupt planetary systems formed with similar stellar densities.

49. Density streams in the disc winds of Classical T Tauri stars

P. P. Petrov, K. N. Grankin, E. V. Babina, S. A. Artemenko, M. M. Romanova, S. Yu. Gorda, A. A. Djupvik, J. F. Gameiro ★ Spectral and photometric variability of the Classical T Tauri stars RY Tau and SU Aur from 2013 to 2022 is analyzed. We find that in SU Aur the H-alpha line's flux at radial velocity RV = -50 +- 7 km/s varies with a period P = 255 +- 5 days. A similar effect previously discovered in RY Tau is confirmed with these new data: P = 21.6 days at RV = -95 +- 5 km/s. In both stars, the radial velocity of these variations, the period, and the mass of the star turn out to be related by Kepler's law, suggesting structural features on the disc plane orbiting at radii of 0.2 AU in RY Tau and 0.9 AU in SU Aur, respectively. Both stars have a large inclination of the accretion disc to the line of sight - so that the line of sight passes through the region of the disc wind. We propose there is an azimuthal asymmetry in the disc wind, presumably in the form of 'density streams', caused by substructures of the accretion disc surface. These streams cannot dissipate until they go beyond the Alfven surface in the disc's magnetic field. These findings open up the possibility to learn about the structure of the inner accretion disc of CTTS on scales less than 1 AU and to reveal the orbital distances related to the planet's formation.

50. Star cluster progenitors are dynamically decoupled from their parent molecular clouds

Nicolas Peretto, Andrew J. Rigby, Fabien Louvet, Gary A. Fuller, Alessio Traficante, Mathilde Gaudel ★ The formation of stellar clusters dictates the pace at which galaxies evolve, and solving the question of their formation will undoubtedly lead to a better understanding of the Universe as a whole. While it is well known that star clusters form within parsec-scale over-densities of interstellar molecular gas called clumps, it is, however, unclear whether these clumps represent the high-density tip of a continuous gaseous flow that gradually leads towards the formation of stars, or a transition within the gas physical properties. Here, we present a unique analysis of a sample of 27 infrared dark clouds embedded within 24 individual molecular clouds that combine a large set of observations, allowing us to compute the mass and velocity dispersion profiles of each, from the scale of tens of parsecs down to the scale of tenths of a parsec. These profiles reveal that the vast majority of the clouds, if not all, are consistent with being self-gravitating on all scales, and that the clumps, on parsec-scale, are often dynamically decoupled from their surrounding molecular clouds, exhibiting steeper density profiles ($\rho \propto r^{-2}$) and flat velocity dispersion profiles ($\sigma \propto r^{0}$), clearly departing from Larson's relations. These findings suggest that the formation of star clusters correspond to a transition regime within the properties of the self-gravitating molecular gas. We propose that this transition regime is one that corresponds to the gravitational collapse of parsec-scale clumps within otherwise stable molecular clouds.

51. Isotopic enrichment of planetary systems from Asymptotic Giant Branch stars

Richard J. Parker, Christina Schoettler ★ Short-lived radioisotopes, in particular 26-Al and 60-Fe, are thought to contribute to the internal heating of the Earth, but are significantly more abundant in the Solar System compared to the Interstellar Medium. The presence of their decay products in the oldest Solar System objects argues for their inclusion in the Sun's protoplanetary disc almost immediately after the star formation event that formed the Sun. Various scenarios have been proposed for their delivery to the Solar System, usually involving one or more core-collapse supernovae of massive stars. An alternative scenario involves the young Sun encountering an evolved Asymptotic Giant Branch (AGB) star. AGBs were previously discounted as a viable enrichment scenario for the Solar System due to the presumed low probability of an encounter between an old, evolved star and a young pre-main sequence star. We report the discovery in Gaia data of an interloping AGB star in the star-forming region NGC2264, demonstrating that old, evolved stars can encounter young forming planetary systems. We use simulations to calculate the yields of 26-Al and 60-Fe from AGBs and their contribution to the long-term geophysical heating of a planet, and find that these are comfortably within the range previously calculated for the Solar System.

52. On the origin of planetary-mass objects in NGC1333

Richard J. Parker, Catarina Alves de Oliveira ★ The dominant formation mechanism of brown dwarfs and planetary mass objects in star-forming regions is presently uncertain. Do they form like stars, via the collapse and fragmentation of cores in Giant Molecular clouds, or do they form like planets in the discs around stars and are ejected via dynamical interactions? In this paper, we quantify the spatial distribution of substellar objects in NGC1333, in particular focusing on planetary-mass objects that have been the target of recent deep imaging observations. We find that these objects have a spatial distribution that is indistinguishable from the stars, and more massive brown dwarfs. We also analyse N-body simulations and find that a population of ejected planets would have a significantly different spatial and kinematic distribution to stars, and brown dwarfs that also formed through gravitational collapse and fragmentation. We therefore conclude that the low-mass substellar objects in NGC1333 formed more like stars than planets, although we predict that a population of hitherto undetected ejected planetary mass objects may be lurking in this, and other star-forming regions.

53. Photoevaporation versus enrichment in the cradle of the Sun

Miti Patel, Cheyenne K. M. Polius, Matthew Ridsdill-Smith, Tim Lichtenberg, Richard Parker ★ The presence of short-lived radioisotopes (SLRs) 26-Al and 60-Fe in the Solar system places constraints on the initial conditions of our planetary system. Most theories posit that the origin of 26-Al and 60-Fe is in the interiors of massive stars, and they are either delivered directly to the protosolar disc from the winds and supernovae of the massive stars, or indirectly via a sequential star formation event. However, massive stars that produce SLRs also emit photoionising far and extreme ultraviolet radiation, which can destroy the gas component of protoplanetary discs, possibly precluding the formation of gas giant planets like Jupiter and Saturn. Here, we perfom N-body simulations of star-forming regions and determine whether discs that are enriched in SLRs can retain enough gas to form Jovian planets. We find that discs are enriched and survive the photoionising radiation only when the dust radius of the disc is fixed and not allowed to move inwards due to the photoevaporation, or outwards due to viscous spreading. Even in this optimal scenario, not enough discs survive until the supernovae of the massive stars and so have zero or very little enrichment in 60-Fe. We therefore suggest that the delivery of SLRs to the Solar system may not come from the winds and supernovae of massive stars.

54. Linking ice and gas in the Coronet cluster in Corona Australis

G. Perotti, J. K. Jørgensen, W. R. M. Rocha, A. Plunkett, E. Artur de la Villarmois, L. E. Kristensen, M. Sewiło, P. Bjerkeli, H. J. Fraser, S. B. Charnley ★ During the journey from the cloud to the disc, the chemical composition of the protostellar envelope material can be either preserved or processed to varying degrees depending on the surrounding physical environment. This works aims to constrain the interplay of solid (ice) and gaseous methanol (CH_3OH) in the outer regions of protostellar envelopes located in the Coronet cluster in Corona Australis (CrA), and assess the importance of irradiation by the Herbig Ae/Be star R CrA. CH_3OH is a prime test-case as it predominantly forms as a consequence of the solid-gas interplay (hydrogenation of condensed CO molecules onto the grain surfaces) and it plays an important role in future complex molecular processing. We present 1.3 mm Submillimeter Array (SMA) and Atacama Pathfinder Experiment (APEX) observations towards the envelopes of four low-mass protostars in the Coronet. Eighteen molecular transitions of seven species are identified. We calculate CH_3OH gas-to-ice ratios in this strongly irradiated cluster and compare them with ratios determined towards protostars located in less irradiated regions such as the Serpens SVS 4 cluster in Serpens Main and the Barnard 35A cloud in the λ Orionis region. The CH_3OH gas-to-ice ratios in the Coronet vary by one order of magnitude (from 1.2×10^{-4} to 3.1×10^{-3}) which is similar to less irradiated regions as found in previous studies. We find that the CH_3OH gas-to-ice ratios estimated in these three regions are remarkably similar despite the different UV radiation field intensities and formation histories. This result suggests that the overall CH_3OH chemistry in the outer regions of low-mass envelopes is relatively independent of variations in the physical conditions and hence that it is set during the prestellar stage.

55. An inner warp discovered in the disk around HD 110058 using VLT/SPHERE and HST/STIS

S. Stasevic, J. Milli, J. Mazoyer, A. -M. Lagrange, M. Bonnefoy, V. Faramaz-Gorka, F. Ménard, A. Boccaletti, E. Choquet, L. Shuai, J. Olofsson, A. Chomez, B. Ren, P. Rubini, C. Desgrange, R. Gratton, G. Chauvin, A. Vigan, E. Matthews ★ An edge-on debris disk was detected in 2015 around the young, nearby A0V star HD 110058. The disk showed features resembling those seen in the disk of beta Pictoris that could indicate the presence of a perturbing planetary-mass companion in the system. We investigated new and archival scattered light images of the disk in order to characterise its morphology and spectrum. In particular, we analysed the disk's warp to constrain the properties of possible planetary perturbers. Our work uses data from two VLT/SPHERE observations and archival data from HST/STIS. We measured the morphology of the disk by analysing vertical profiles along the length of the disk to extract the centroid spine position and vertical height. We extracted the surface brightness and reflectance spectrum of the disk. We detect the disk between 20 au (with SPHERE) and 150 au (with STIS), at a position angle of $159.6^\circ\pm0.6^\circ$. Analysis of the spine shows an asymmetry between the two sides of the disk, with a 3.4°±0.9° warp between 20 au and 60 au. The disk is marginally vertically resolved in scattered light, with a vertical aspect ratio of 9.3±0.7% at 45 au. The extracted reflectance spectrum is featureless, flat between 0.95 micron and 1.1 micron, and red from 1.1 micron to 1.65 micron. The outer parts of the disk are also asymmetric with a tilt between the two sides compatible with a disk made of forward-scattering particles and seen not perfectly edge-on, suggesting an inclination of <84°. The presence of an undetected planetary-mass companion on an inclined orbit with respect to the disk could explain the warp. The misalignment of the inner parts of the disk with respect to the outer disk suggests a warp that has not yet propagated to the outer parts of the disk, favouring the scenario of an inner perturber as the origin of the warp.

56. Sublimation of refractory minerals in the gas envelopes of accreting rocky planets

Marie-Luise Steinmeyer, Peter Woitke, Anders Johansen ★ Protoplanets growing within the protoplanetary disk by pebble accretion acquire hydrostatic gas envelopes. Due to accretion heating, the temperature in these envelopes can become high enough to sublimate refractory minerals which are the major components of the accreted pebbles. Here we study the sublimation of different mineral species and determine whether sublimation plays a role during the growth by pebble accretion. For each snapshot in the growth process, we calculate the envelope structure and sublimation temperature of a set of mineral species representing different levels of volatility. Sublimation lines are determined using and equilibrium scheme for the chemical reactions responsible for destruction and formation of the relevant minerals. We find that the envelope of the growing planet reaches temperatures high enough to sublimate all considered mineral species when the mass is larger than 0.4 Earth masses. The sublimation lines are located within the gravitionally bound envelope of the planet. We make a detailed analysis of the sublimation of FeS at around 720 K, beyond which the mineral is attacked by H2 to form gaseous H2S and solid Fe. We calculate the sulfur concentration in the planet under the assumption that all sulfur released as H2S is lost from the planet by diffusion back to the protoplanetary disk. Our calculated values are in good agreement with the slightly depleted sulfur abundance of Mars, while the model overpredicts the extensive sulfur depletion of Earth by a factor of approximately 2. We show that a collision with a sulfur-rich body akin to Mars in the moon-forming impact lifts the Earth's sulfur abundance to approximately 10% of the solar value for all impactor masses above 0.05 Earth masses.

57. X-ray emission from pre-main sequence stars with multipolar magnetic fields

Kieran A. Stuart, Scott G. Gregory ★ The large-scale magnetic fields of several pre-main sequence (PMS) stars have been observed to be simple and axisymmetric, dominated by tilted dipole and octupole components. The magnetic fields of other PMS stars are highly multipolar and dominantly non-axisymmetric. Observations suggest that the magnetic field complexity increases as PMS stars evolve from Hayashi to Henyey tracks in the Hertzsprung–Russell diagram. Independent observations have revealed that X-ray luminosity decreases with age during PMS evolution, with Henyey track PMS stars having lower fractional X-ray luminosities (L_X/L_*) compared to Hayashi track stars. We investigate how changes in the large-scale magnetic field topology of PMS stars influences coronal X-ray emission. We construct coronal models assuming pure axisymmetric multipole magnetic fields, and magnetic fields consisting of a dipole plus an octupole component only. We determine the closed coronal emitting volume, over which X-ray emitting plasma is confined, using a pressure balance argument. From the coronal volumes we determine X-ray luminosities. We find that L_X decreases as the degree ℓ of the multipole field increases. For dipole plus octupole magnetic fields we find that L_X tends to decrease as the octupole component becomes more dominant. By fixing the stellar parameters at values appropriate for a solar mass PMS star, varying the magnetic field topology results in two orders of magnitude variation in L_X. Our results support the idea that the decrease in L_X as PMS stars age can be driven by an increase in the complexity of the large-scale magnetic field.

58. An ALMA Glimpse of Dense Molecular Filaments Associated with High-mass Protostellar Systems in the Large Magellanic Cloud

Kazuki Tokuda, Naoto Harada, Kei E. I. Tanaka, Tsuyoshi Inoue, Takashi Shimonishi, Yichen Zhang, Marta Sewiło, Yuri Kunitoshi, Ayu Konishi, Yasuo Fukui, Akiko Kawamura, Toshikazu Onishi, Masahiro N. Machida ★ Recent millimeter/sub-millimeter facilities have revealed the physical properties of filamentary molecular clouds in relation to high-mass star formation. A uniform survey of the nearest, face-on star-forming galaxy, the Large Magellanic Cloud (LMC), complements the Galactic knowledge. We present ALMA survey data with a spatial resolution of ∼0.1 pc in the 0.87 mm continuum and HCO^+(4-3) emission toward 30 protostellar objects with luminosities of 10^4-$10^{5.5}$ $L_\odot$ in the LMC. The spatial distributions of the HCO^+(4-3) line and thermal dust emission are well correlated, indicating that the line effectively traces dense, filamentary gas with an H_2 volume density of $\gtrsim 10^5$ cm^{-3} and a line mass of $\sim 10^3$-10^4 $M_\odot$ pc^{-1}. Furthermore, we obtain an increase in the velocity linewidths of filamentary clouds, which follows a power-law dependence on their H_2 column densities with an exponent of ∼0.5. This trend is consistent with observations toward filamentary clouds in nearby star-forming regions withiin $\lesssim$1 kpc from us and suggests enhanced internal turbulence within the filaments owing to surrounding gas accretion. Among the 30 sources, we find that 14 are associated with hub-filamentary structures, and these complex structures predominantly appear in protostellar luminosities exceeding $\sim 5\times 10^4$ $L_\odot$. The hub-filament systems tend to appear in the latest stages of their natal cloud evolution, often linked to prominent H II regions and numerous stellar clusters. Our preliminary statistics suggest that the massive filaments accompanied by hub-type complex features may be a necessary intermediate product in forming extremely luminous high-mass stellar systems capable of ultimately dispersing the parent cloud.

59. Photometric determination of the mass accretion rates of pre-main sequence stars. VII. The low-density cluster NGC 376 in the Small Magellanic Cloud

Styliani Tsilia, Guido De Marchi, Nino Panagia ★ Aims. We study the properties of low-mass stars recently formed in the field of the NGC 376 cluster in the Small Magellanic Cloud (SMC). Methods. Using photometric observations acquired with the Hubble Space Telescope (HST) in the V, I and Halpha bands, we identify 244 candidate pre-main sequence (PMS) stars showing Halpha excess emission at the 5 sigma level and with Halpha equivalent width of 20 Å or more. We derive physical parameters for all PMS stars, including masses, ages, and mass accretion rates. We compare the effective mass accretion rate of stars in NGC 376 to that of objects in the NGC 346 cluster, which features similar metallicity but higher total mass and gas density. Results. We find a median age of 28 Myr for this population (with 25 and 75 percentiles at about 20 and 40 Myr, respectively), in excellent agreement with previous studies of massive stars in the same field. The PMS stars are rather uniformly distributed across the field, whereas massive stars are more clustered. The spatial distribution of PMS objects is compatible with them having formed in the centre of the cluster and then migrated outwards. We find that in NGC 376 the mass accretion rate is systematically lower than in NGC 346 for stars of the same mass and age. This indicates that, besides metallicity, there are other environmental factors affecting the rate of mass accretion onto PMS stars. Our observations suggest that the gas density in the star-forming region might play a role.

60. Photometric determination of the mass accretion rates of pre-main-sequence stars. VIII. Recent star formation in NGC 299

Marissa Vlasblom, Guido De Marchi ★ We studied the properties of the young stellar populations in the NGC 299 cluster in the Small Magellanic Cloud using observations obtained with the Hubble Space Telescope in the V, I, and $H\alpha$ bands. We identified 250 stars with Hα excess exceeding 5 σ and an equivalent width of the Hα emission line of at least 20 Å, indicating that these stars are still undergoing accretion and therefore represent bona fide pre-main-sequence (PMS) objects. For 240 of these stars, we derived the mass, age, and mass accretion rate by comparing the observed photometry with theoretical models. We find evidence for the existence of two populations of PMS stars, with median ages of 25 and 50 Myr respectively. The average mass accretion rate for these PMS stars is $\sim 5 \times 10^{-9}$ $M_\odot$ yr^{-1}, which is comparable to the values found in other low-metallicity, low-density clusters in the Magellanic Clouds, but is about a factor of three lower than those measured for stars of similar mass and age in denser Magellanic Cloud stellar regions. Our findings support the hypothesis that both the metallicity and density of the forming environment can affect the mass accretion rate and thus the star formation process in a region. A study of the spatial distribution of both massive stars and (low-mass) PMS objects reveals that the former are clustered near the nominal centre of NGC 299, whereas the PMS stars are rather uniformly distributed over the field. To explore whether the stars formed in an initially more diffuse or compact structure, we studied the cluster's stellar density profile. We find a core radius $r_c \simeq 0.6$ pc and a tidal radius $r_t \simeq 5.5$ pc, with an implied concentration parameter $c \simeq 1$, suggesting that the cluster could be dispersing into the field.

61. Protostellar Interferometric Line Survey of the Cygnus-X region (PILS-Cygnus) – The role of the external environment in setting the chemistry of protostars

S. J. van der Walt, L. E. Kristensen, H. Calcutt, J. K. Jørgensen, R. T. Garrod ★ (Abridged) Molecular lines are commonly detected towards protostellar sources. However, to get a better understanding of the chemistry of these sources we need unbiased molecular surveys over a wide frequency range for as many sources as possible to shed light on the origin of this chemistry, particularly any influence from the external environment. We present results from the PILS-Cygnus survey of ten intermediate- to high-mass protostellar sources in the nearby Cygnus-X complex, through high angular resolution interferometric observations over a wide frequency range. Using the Submillimeter Array (SMA), a spectral line survey of ten sources was performed in the frequency range 329-361 GHz, with an angular resolution of ∼1.5 arcsec, (∼2000 AU, source distance of 1.3 kpc). Spectral modelling was performed to identify molecular emission and determine column densities and excitation temperatures for each source. We detect CH_3OH towards nine of the ten sources, CH_3OCH_3 and CH_3OCHO towards three sources, and CH_3CN towards four sources. Towards five sources the chemistry is spatially differentiated (different species peak at different positions and are offset from the peak continuum emission). The chemical properties of each source do not correlate with their position in the Cygnus-X complex, nor do the distance or direction to the nearest OB associations. However, the five sources located in the DR21 filament do appear to show less line emission compared to the five sources outside the filament. This work shows how important wide frequency coverage observations are combined with high angular resolution observations for studying the protostellar environment. Based on the ten sources observed here, the external environment appears to only play a minor role in setting the chemical environment on these small scales (< 2000 AU).

62. The molecular clouds in a section of the third Galactic quadrant: observational properties and chemical abundance ratio between CO and its isotopologues

Chen Wang, Haoran Feng, Ji Yang, Xuepeng Chen, Yang Su, Qing-Zeng Yan, Fujun Du, Yuehui Ma, Jiajun Cai ★ We compare the observational properties between ^{12}CO, ^{13}CO, and C^{18}O and summarize the observational parameters based on 7069 clouds sample from the Milky Way Imaging Scroll Painting (MWISP) CO survey in a section of the third Galactic quadrant. We find that the ^{13}CO angular area ($A_{^{13}\mathrm{CO}}$) generally increases with that of ^{12}CO ($A_{^{12}\mathrm{CO}}$), and the ratio of $A_{^{13}\mathrm{CO}}$ to $A_{^{12}\mathrm{CO}}$ is 0.38 by linear fitting. We find that the ^{12}CO and ^{13}CO flux are tightly correlated as $F_{^{13}\mathrm{CO}} = 0.17\ F_{^{12}\mathrm{CO}}$ with both fluxes calculated within the ^{13}CO-bright region. This indicates that the abundance $X_{^{13}\mathrm{CO}}$ is a constant to be $6.5^{+0.1}_{-0.5} \times 10^{-7}$ for all samples under assumption of local thermodynamic equilibrium (LTE). Additionally, we observed that the X-factor is approximately constant in large sample molecular clouds. Similarly, we find $F_{\mathrm{C}^{18}\mathrm{O}} = 0.11\ F_{^{13}\mathrm{CO}}$ with both fluxes calculated within C^{18}O-bright region, which indicates that the abundance ratios $X_{^{13}\mathrm{CO}}/X_{\mathrm{C}^{18}\mathrm{O}}$ stays the same value $9.7^{+0.6}_{-0.8}$ across the molecular clouds under LTE assumption. The linear relationships of $F_{^{12}\mathrm{CO}}$ vs. $F_{^{13}\mathrm{CO}}$ and $F_{^{13}\mathrm{CO}}$ vs. $F_{\mathrm{C}^{18}\mathrm{O}}$ hold not only for the ^{13}CO-bright region or C^{18}O-bright region, but also for the entire molecular cloud scale with lower flux ratio. The abundance ratio $X_{^{13}\mathrm{CO}}/X_{\mathrm{C}^{18}\mathrm{O}}$ inside clouds shows a strong correlation with column density and temperature. This indicates that the $X_{^{13}\mathrm{CO}}/X_{\mathrm{C}^{18}\mathrm{O}}$ is dominated by a combination of chemical fractionation, selectively dissociation, and self-shielding effect inside clouds.

63. MAPS: Constraining Serendipitous Time Variability in Protoplanetary Disk Molecular Ion Emission

Abygail R. Waggoner, L. Ilsedore Cleeves, Ryan A. Loomis, Yuri Aikawa, Jaehan Bae, Jennifer B. Bergner, Alice S. Booth, Jenny K. Calahan, Gianni Cataldi, Charles J. Law, Romane Le Gal, Feng Long, Karin I. Öberg, Richard Teague, David J. Wilner ★ Theoretical models and observations suggest that the abundances of molecular ions in protoplanetary disks should be highly sensitive to the variable ionization conditions set by the young central star. We present a search for temporal flux variability of HCO+ J=1-0, which was observed as a part of the Molecules with ALMA at Planet-forming Scales (MAPS) ALMA Large Program. We split out and imaged the line and continuum data for each individual day the five sources were observed (HD 163296, AS 209, GM Aur, MWC 480, and IM Lup, with between 3 to 6 unique visits per source). Significant enhancement ($>3\sigma$) was not observed, but we find variations in the spectral profiles in all five disks. Variations in AS 209, GM Aur, and HD 163296 are tentatively attributed to variations in HCO+ flux, while variations in IM Lup and MWC 480 are most likely introduced by differences in the *uv* coverage, which impact the amount of recovered flux during imaging. The tentative detections and low degree of variability are consistent with expectations of X-ray flare driven HCO+ variability, which requires relatively large flares to enhance the HCO+ rotational emission at significant (>20%) levels. These findings also demonstrate the need for dedicated monitoring campaigns with high signal to noise ratios to fully characterize X-ray flare driven chemistry.

64. The Accretion History of EX Lup: A Century of Bursts, Outbursts, and Quiescence

Mu-Tian Wang, Gregory J. Herczeg, Hui-Gen Liu, Min Fang, Doug Johnstone, Ho-Gyu Lee, Frederick M. Walter, Franz-Josef Hambsch, Carlos Contreras Pena, Jeong-Eun Lee, Mervyn Millward, Andrew Pearce, Berto Monard, Lihang Zhou ★ EX Lup is the archetype for the class of young stars that undergoes repeated accretion outbursts of ~ 5 mag at optical wavelengths and that last for months. Despite extensive monitoring that dates back 130 years, the accretion history of EX Lup remains mostly qualitative and has large uncertainties. We assess historical accretion rates of EX Lup by applying correlations between optical brightness and accretion, developed on multi-band magnitude photometry of the ~ 2 mag optical burst in 2022. Two distinct classes of bursts occur: major outbursts ($\Delta V \sim 5$ mag) have year-long durations, are rare, reach accretion rates of $\dot{M}_{\mathrm{acc}} \sim 10^{-7}\ M_\odot\ \mathrm{yr}^{-1}$ at peak, and have a total accreted mass of around 0.1 Earth masses. The characteristic bursts ($\Delta V \sim 2$ mag) have durations of $\sim 2-3$ months, are more common, reach accretion rates of $\dot{M}_{\mathrm{acc}} \sim 10^{-8}\ M_\odot\ \mathrm{yr}^{-1}$ at peak, and have a total accreted mass of around 10^{-3} Earth masses. The distribution of total accreted mass in the full set of bursts is poorly described by a power law, which suggests different driving causes behind the major outburst and characteristic bursts. The total mass accreted during two classes of bursts is around two times the masses accreted during quiescence. Our analysis of the light curves reveals a color-dependent time lag in the 2022 post-burst light curve, attributed to the presence of both hot and cool spots on the stellar surface.

65. ALMA observations of the Extended Green Object G19.01−0.03: II. A massive protostar with typical chemical abundances surrounded by four low-mass prestellar core candidates

Gwenllian M. Williams, Claudia J. Cyganowski, Crystal L. Brogan, Todd R. Hunter, Pooneh Nazari, Rowan J. Smith ★ We present a study of the physical and chemical properties of the Extended Green Object (EGO) G19.01−0.03 using sub-arcsecond angular resolution Atacama Large Millimeter/submillimeter Array (ALMA) 1.05mm and Karl G. Jansky Very Large Array (VLA) 1.21cm data. G19.01−0.03 MM1, the millimetre source associated with the central massive young stellar object (MYSO), appeared isolated and potentially chemically young in previous Submillimeter Array observations. In our $\sim 0.4''$-resolution ALMA data, MM1 has four low-mass millimetre companions within 0.12pc, all lacking maser or outflow emission, indicating they may be prestellar cores. With a rich ALMA spectrum full of complex organic molecules, MM1 does not appear chemically young, but has molecular abundances typical of high-mass hot cores in the literature. At the 1.05mm continuum peak of MM1, N(CH_3OH) = $(2.22 \pm 0.01) \times 10^{18}$cm^{-2} and $T_{\rm ex} = 162.7^{+0.3}_{-0.5}$K based on pixel-by-pixel Bayesian analysis of LTE synthetic methanol spectra across MM1. Intriguingly, the peak CH_3OH $T_{\rm ex} = 165.5 \pm 0.6$ K is offset from MM1's millimetre continuum peak by $0.22'' \sim 880$au, and a region of elevated CH_3OH $T_{\rm ex}$ coincides with free-free VLA 5.01cm continuum, adding to the tentative evidence for a possible unresolved high-mass binary in MM1. In our VLA 1.21cm data, we report the first NH_3(3,3) maser detections towards G19.01−0.03, along with candidate 25GHz CH_3OH $5(2,3) - 5(1,4)$ maser emission; both are spatially and kinematically coincident with 44GHz Class I CH_3OH masers in the MM1 outflow. We also report the ALMA detection of candidate 278.3GHz Class I CH_3OH maser emission towards this outflow, strengthening the connection of these three maser types to MYSO outflows.

66. CMR exploration II – filament identification with machine learning

Duo Xu, Shuo Kong, Avichal Kaul, Hector G. Arce, Volker Ossenkopf-Okada ★ We adopt magnetohydrodynamics (MHD) simulations that model the formation of filamentary molecular clouds via the collision-induced magnetic reconnection (CMR) mechanism under varying physical conditions. We conduct radiative transfer using RADMC-3D to generate synthetic dust emission of CMR filaments. We use the previously developed machine learning technique CASI-2D along with the diffusion model to identify the location of CMR filaments in dust emission. Both models showed a high level of accuracy in identifying CMR filaments in the test dataset, with detection rates of over 80% and 70%, respectively, at a false detection rate of 5%. We then apply the models to real Herschel dust observations of different molecular clouds, successfully identifying several high-confidence CMR filament candidates. Notably, the models are able to detect high-confidence CMR filament candidates in Orion A from dust emission, which have previously been identified using molecular line emission.

67. On the conditions for warping and breaking protoplanetary discs

Alison K. Young, Struan Stevenson, C. J. Nixon, Ken Rice ★ Recent observations demonstrate that misalignments and other out-of-plane structures are common in protoplanetary discs. Many of these have been linked to a central host binary with an orbit that is inclined with respect to the disc. We present simulations of misaligned circumbinary discs with a range of parameters to gain a better understanding of the link between those parameters and the disc morphology in the wave-like regime of warp propagation that is appropriate to protoplanetary discs. The simulations confirm that disc tearing is possible in protoplanetary discs as long as the mass ratio, μ, and disc-binary inclination angle, i, are not too small. For the simulations presented here this corresponds to $\mu > 0.1$ and $i \gtrsim 40^\circ$. For highly eccentric binaries, tearing can occur for discs with smaller misalignment. Existing theoretical predictions provide an estimate of the radial extent of the disc in which we can expect breaking to occur. However, there does not seem to be a simple relationship between the disc properties and the radius within the circumbinary disc at which the breaks appear, and furthermore the radius at which the disc breaks can change as a function of time in each case. We discuss the implications of our results for interpreting observations and suggest some considerations for modelling misaligned discs in the future.

68. ATLASGAL: 3-mm class I methanol masers in high-mass star formation regions

W. Yang, Y. Gong, K. M. Menten, J. S. Urquhart, C. Henkel, F. Wyrowski, T. Csengeri, S. P. Ellingsen, A. R. Bemis, J. Jang ★ We analyzed the 3-mm wavelength spectral line survey of 408 ATLASGAL clumps observed with the IRAM 30m-telescope, focusing on the class I methanol masers with frequencies near 84, 95 and 104.3 GHz. We detect narrow, maser-like features towards 54, 100 and 4 sources in the maser lines near 84, 95 and 104.3 GHz, respectively. Among them, fifty 84 GHz masers, twenty nine 95 GHz masers and four rare 104.3 GHz masers are new discoveries. The new detections increase the number of known 104.3 GHz masers from 5 to 9. The 95 GHz class I methanol maser is generally stronger than the 84 GHz maser counterpart. We find 9 sources showing class I methanol masers but no SiO emission, indicating that class I methanol masers might be the only signpost of protostellar outflow activity in extremely embedded objects at the earliest evolutionary stage. Class I methanol masers that are associated with sources that show SiO line wings are more numerous and stronger than those without such wings. The total integrated intensity of class I methanol masers is well correlated with the integrated intensity and velocity coverage of the SiO (2–1) emission. The properties of class I methanol masers are positively correlated with the bolometric luminosity, clump mass, peak H_2 column density of their associated clumps but uncorrelated with the luminosity-to-mass ratio, dust temperature, and mean H_2 volume density. We suggest that the properties of class I masers are related to shocks traced by SiO. Based on our observations, we conclude that class I methanol masers at 84 and 95 GHz can trace a similar evolutionary stage as H_2O maser, and appear prior to 6.7 and 12.2 GHz methanol and OH masers. Despite their small number, the 104.3 GHz class I masers appear to trace a short and more evolved stage compared to the other class I masers. [abridged]

69. Buoyancy response of a disk to an embedded planet: a cross-code comparison at high resolution

Alexandros Ziampras, Sijme-Jan Paardekooper, Richard P. Nelson ★ In radiatively inefficient, laminar protoplanetary disks, embedded planets can excite a buoyancy response as gas gets deflected vertically near the planet. This results in vertical oscillations that drive a vortensity growth in the planet's corotating region, speeding up inward migration in the type-I regime. We present a comparison between PLUTO/IDEFIX and FARGO3D using 3D, inviscid, adiabatic numerical simulations of planet-disk interaction that feature the buoyancy response of the disk, and show that PLUTO/IDEFIX struggle to resolve higher-order modes of the buoyancy-related oscillations, weakening vortensity growth and the associated torque. We interpret this as a drawback of total-energy-conserving, finite-volume schemes. Our results indicate that a very high resolution or high-order scheme is required in shock-capturing codes in order to adequately capture this effect.